

EXHIBIT A

**UNITED STATES DISTRICT COURT
DISTRICT OF MINNESOTA**

IN RE: Bair Hugger Forced Air Warming
Products Liability Litigation

Case No. 0:16-cv-04159 (JNE/DTS)

This Document Relates to All Actions.

**PLAINTIFF'S SUPPLEMENTAL
EXPERT REPORT**

PLAINTIFF(S)

ADA TROMBLEY

VS.

**3M COMPANY,
a Delaware Corporation**

Plaintiff herewith submits the supplemental report of Nathan Bushnell, Ph.D. in order to reserve all rights and preserve the record in this and other cases in this MDL.

Professional Background

I am the Mid-west and Texas Engineering Lead Engineer for SimuTech Group. SimuTech Group is the largest reseller of ANSYS product in North America. SimuTech Group is an elite ANSYS Channel partner.

In my roles at SimuTech including as a Lead Engineer, I have performed more than 50 external consulting projects using a variety of advanced Computation Fluid Dynamic (CFD) techniques for many different industries. Computation Fluid Dynamics uses computers to calculate fluid motion by solving a set of equations based on the fundamental laws of physics. My engineering expertise includes CFD Modeling of many different situations including Multiphase and Turbulent Fluid Flows. Also, I teach both public/project specific CFD training and provide technical CFD support to various professional engineers on a multitude of fluid dynamics topics. I am an ANSYS Certified Professional, Fluid Technical.

I gained my Ph.D. in Chemical and Process Engineering from the University of Canterbury in New Zealand.

Refer to Appendix I for my complete Resume.

Summary

John Abraham, Ph.D.'s CFD modeling does not support his conclusions because there are numerous errors in his CFD models. The errors are as follows:

- Dr. Abraham erred by using a steady state streamline on a single transient result. Streamlines require a steady state solution to be accurate, and the transient model Dr. Abraham used is not steady. It can clearly be shown the results will change depending on which result he chooses to use.
- Dr. Abraham erred by not running his transient model long enough. Dr. Abraham's model ran for 1.2 seconds (Bair Hugger 750 model) and 5.07 seconds (Bair Hugger 505 model) of simulation time. The model did not run long enough to predict the fluid motion in the operating room as he has defined it. The results can be shown to be dependent on the definition of his unknown initial condition.
- Dr. Abraham uses results from a model that will diverge. This is outside standard industry practices and highly likely to give inaccurate results.
- Dr. Abraham uses a mesh that is under resolved and has unacceptable quality elements, thus resulting in incorrect results. If he refined his mesh he would get different results.
- Dr. Abraham used a high-resolution scheme with his LES which is known to cause errors in the solution.
- Dr. Abraham used streamlines, he should have used particle tracking. Particle tracking is significantly more accurate and the industry standard approach to particle distribution problems. Further, the question that is at issue is particle location, not streamlines.
- Dr. Abraham does not support any of his assumptions with any sensitivity analysis.

- Dr. Abraham's validation is not document enough to be confirmed by his results, also his choice of validation does not prove the accuracy of his methodology of a steady state streamline on a single transient timestep to accurately particle motion.
- Dr. Abraham has numerous changes (and assumptions) to his model that are undocumented and have no justification greatly reducing any confidence in modeling process undertaken by him.

Overview of CFD

Computational fluid dynamics (CFD) is an advanced engineering method for calculating flow. CFD is a branch of fluid mechanics that uses numerical methods and algorithms to solve problems that involve fluid flows. These problems can be either flow within a confined space, external flow around a solid body, or a combination of both.

The governing equations for CFD are derived from basic principles of physics, including the conservation of mass, energy and Newton's second Law of motion. Almost all CFD models use a set of governing equations for mass and momentum, with additional equations as needed, such as turbulent flow, multi-phase flow, reactions, combustion, equations of state, etc. The flow region that is to be analyzed is subdivided into many small elements. The CFD solution process is an iterative procedure where the governing equations are simultaneously solved for the numerous individual elements. Computers perform these numerous calculations.

The governing equations that describe the momentum transfer in Newtonian fluid are called the Navier-Stokes equations. A Newtonian fluid is one where the shear stress is linearly proportional to the velocity gradient. Many common fluids such as air, water, oil, and gasses meet the criteria for a Newtonian fluid. The principal equations solved in almost all CFD models are the Navier-Stokes equations combined with the conservation of mass equation. The Navier-Stokes equations were first derived in the first half of the nineteenth century. Numerical techniques are required to solve them, except for some special cases, due to the complexity of the mathematical equations.

CFD Methodology

- The basic process for a CFD analysis is as follows. First, a geometric model is developed that defines the fluid flow passage. The geometric model includes the smallest details which influence the flow.
- The model is then subdivided into smaller discrete cells (mesh). The mesh may be uniform or non-uniform.
- The Navier-Stokes equations, conservation of mass, and the appropriate modeling equations necessary for a specific application (such as: conservation of energy, turbulence, etc.) are defined throughout the model.
- The material properties of the fluid(s) modeled are defined.
- Boundary conditions are defined. This involves specifying the fluid behavior and properties at the boundaries of the flow volume.

- The equations are then solved using an iterative procedure. The iterative method is based upon numerical techniques and involves changing the values at each mesh cell until the values correctly give agreement based on the equations defined by the model. The solution is then considered “converged.”
- Finally, a postprocessor is used for the analysis and visualization of the resulting solution.
- Additionally, the model is then resolved to gain an understanding of the impact of modeling inputs by undertaking sensitivity studies.

Fee Schedule

SimuTech Group, Inc. for whom I work is being compensated by Kennedy Hodges L.L.C. My company's compensation rate is \$250 per hour for work outside of Deposition and Trail appearances. For Deposition and Trail appearances my company's compensation rate is \$500 per hour. Plus, reimbursements for direct expenses.

Review

My comments and opinions are based on my review of the CFX transient files Abraham00000001.trn and 2540_full.trn as they relate to the Abraham Expert Report.pdf provided by Dr. Abraham. In addition, I also reviewed the Abraham00000003 (2).agdb file CAD file.

No sensitivity testing

Due to the highly nonlinear nature of fluid problem, sensitivity testing is typically performed to check the impact of modeling assumptions. Dr. Abraham also gives a comparative statement, (*"that forced-air patient warming does not meaningfully impact air flow currents in operating room"*), however he does not have any baseline models to compare against, so he can only guess at what the air flow patterns would be like with the Bair Hugger turn off. He also doesn't look at any effect of people being in the operating room.

Dr. Abraham assumptions in his modeling approach are also not supported with any sensitivity analysis, to test the validity of his assumptions.

Transient modeling

Transient models change with time. Transient modeling is not unique to CFD, it is a common technique across engineering.

The underlying equations that define fluid motion are transient. Steady state modeling is a simplification that can only be accurately when the flow is not changing with time.

A transient CFD model is defined by a set of initial condition that define the original state of the fluid system and then the model is solved for a specific duration defined by the user.

During a transient solution the solver will produce information at each node of the mesh at each timestep that can be post processed. For practicable reasons (like hard drive space), the user might choose to write the information to hard drive only periodically. The *.trn files provided by Dr. Abraham are the transient result files generated at a specific time.

Initial Conditions are not defined

Dr. Abraham does not state what his initial conditions the model definition is incomplete without it and it is unclear what he modeled.

Transient Duration

Dr. Abraham makes an error by not running his transient models long enough. Dr. Abraham models were only run for 1.2s and 5.07s for Abraham0000001.trn and 2540_full.trn respectively (Figures 1 and 2).

Transient model results are dependent on the initial conditions particularly given the short duration of his transient solution, the solution is highly dependent on the unknown initial conditions and not by the stated model definition. Figures 3 through 7 show the temperature contour. Although streamlines were added to give an approximate understanding relative distance the air could have traveled given the time solved and the speed of the air movement in the room, a more accurate method would be to use the industry standard approach to look at the solution with some combination of contour plots and/or monitor plots, however since on the single transient result files was only available, this is not possible. Figures 8 and 9 show the velocity contour and streamlines from the inlet.

Outline	Variables	Expressions	Calculators	Turbo
Expressions				
		Accumulated Time Step	264	
		Current Time Step	264	
		Reference Pressure	1 [atm]	
		Sequence Step	264	
		Time	1.2 [s]	
		atstep	Accumulated Time Step	
		ctstep	Current Time Step	
		sstep	Sequence Step	
		t	Time	

Figure 1 Timestep and time information from Abraham0000001.trn

Outline	Variables	Expressions	Calculators	Turbo
Expressions				
		Accumulated Time Step	2540	
		Current Time Step	2540	
		Reference Pressure	1 [atm]	
		Sequence Step	2540	
		Time	5.07 [s]	
		atstep	Accumulated Time Step	
		ctstep	Current Time Step	
		sstep	Sequence Step	
		t	Time	

Figure 2 Timestep and time information from 2540_full.trn

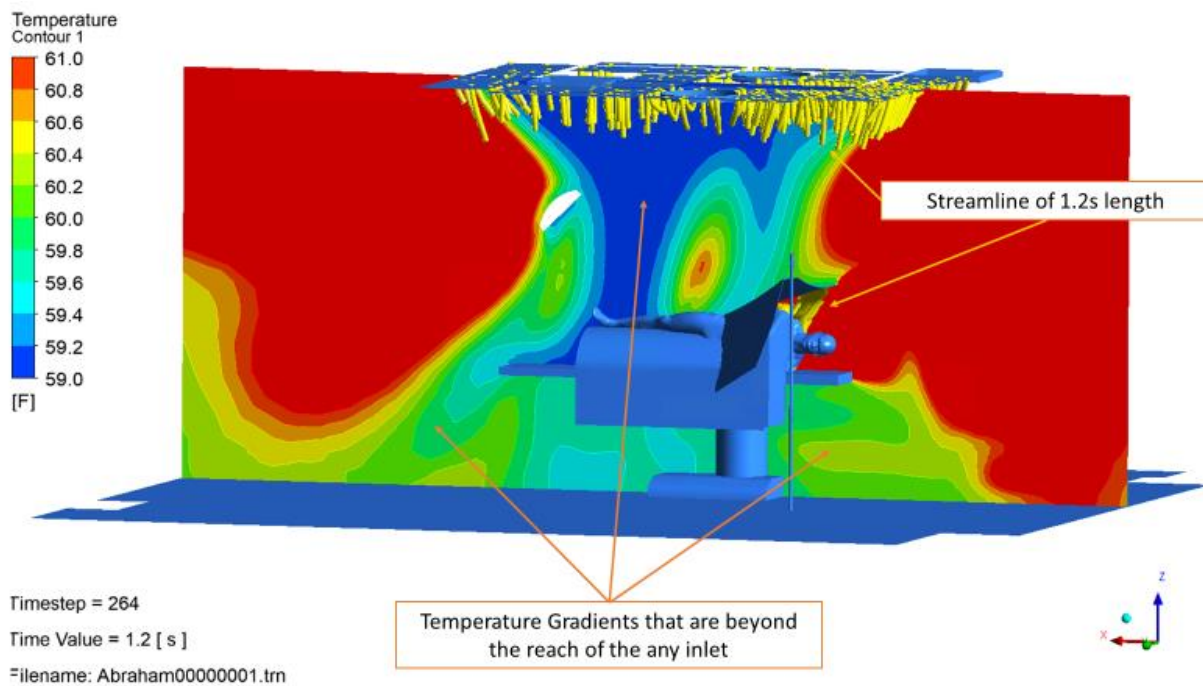


Figure 3 The temperature is contour plotted on a plane at $y = -3.85986$ (m), with the scale trimmed to 59.0 ($^{\circ}\text{F}$) and 61 ($^{\circ}\text{F}$) for the Abraham00000001.trn results. Yellow streamlines are added to show approximately the distance the inlet flows traveled in 1.2 (s).

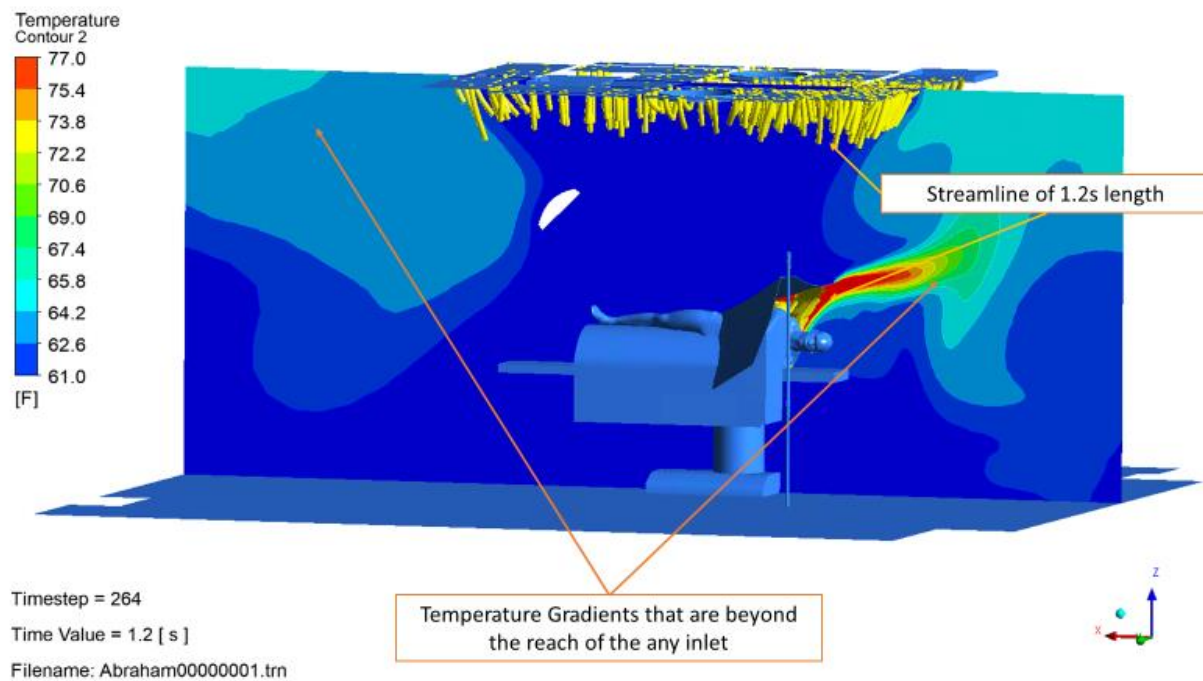


Figure 4 The temperature is contour plotted on a plane at $y = -3.85986$ (m), with the scale trimmed to 61 (°F) and 77 (°F) for the Abraham00000001.trn results. Yellow streamlines are added to show approximately the distance the inlet flows traveled in 1.2 (s).

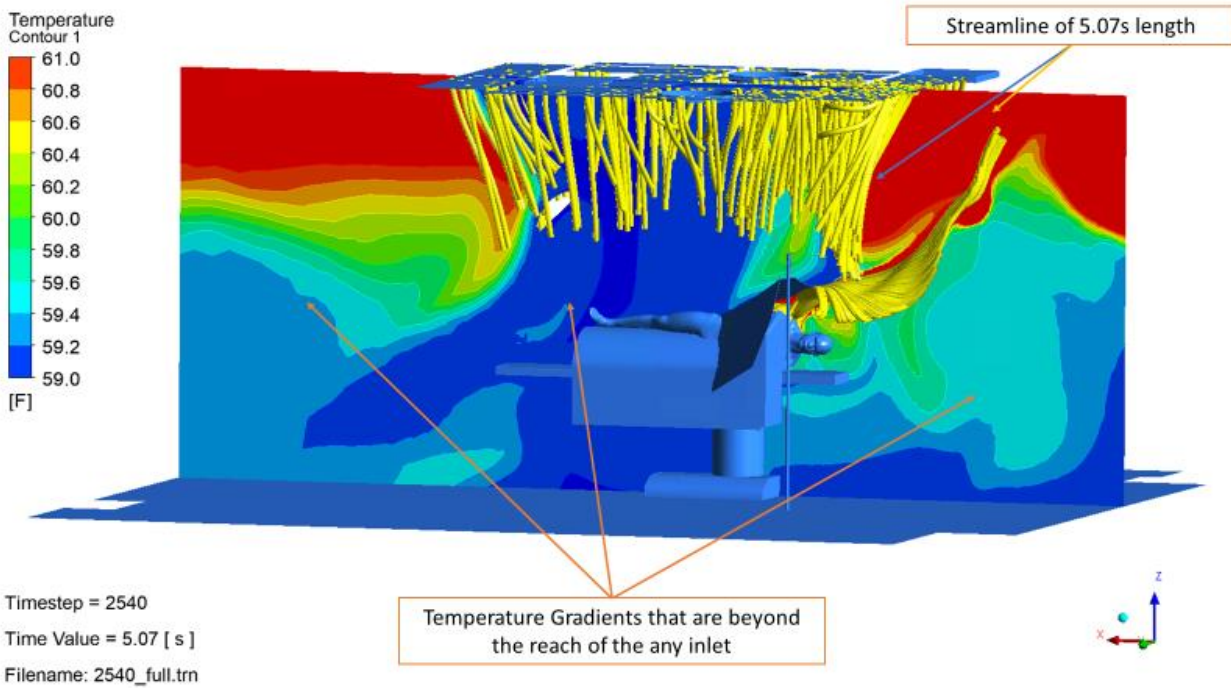


Figure 5 The temperature is contour plotted on a plane at $y = -3.85986$ (m), with the scale trimmed to 59.0 (°F) and 61 (°F) for the 2540_full.trn results. Yellow streamlines are added to show approximately the distance the inlet flows traveled in 5.07 (s).

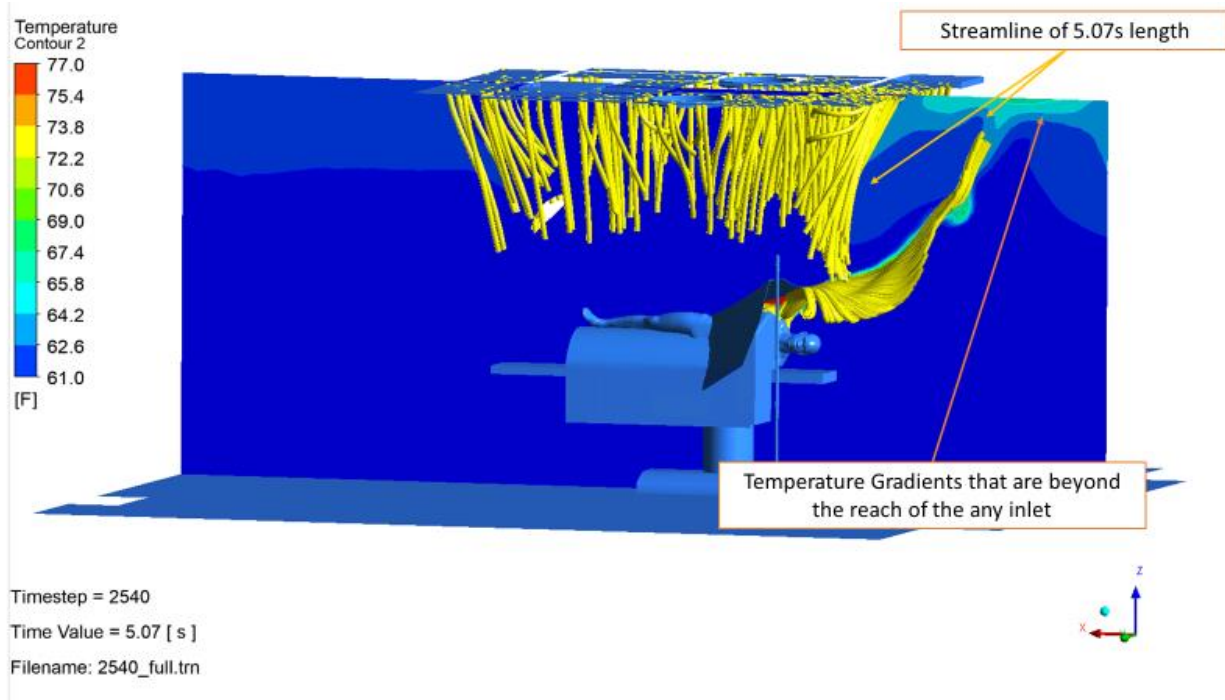


Figure 6 The temperature is contour plotted on a plane at $y = -3.85986$ m, with the scale trimmed to 61.0 (°F) and 77 (°F) for the 2540_full.trn results. Yellow streamlines are added to show approximately the distance the inlet flows traveled in 1.2 (s).

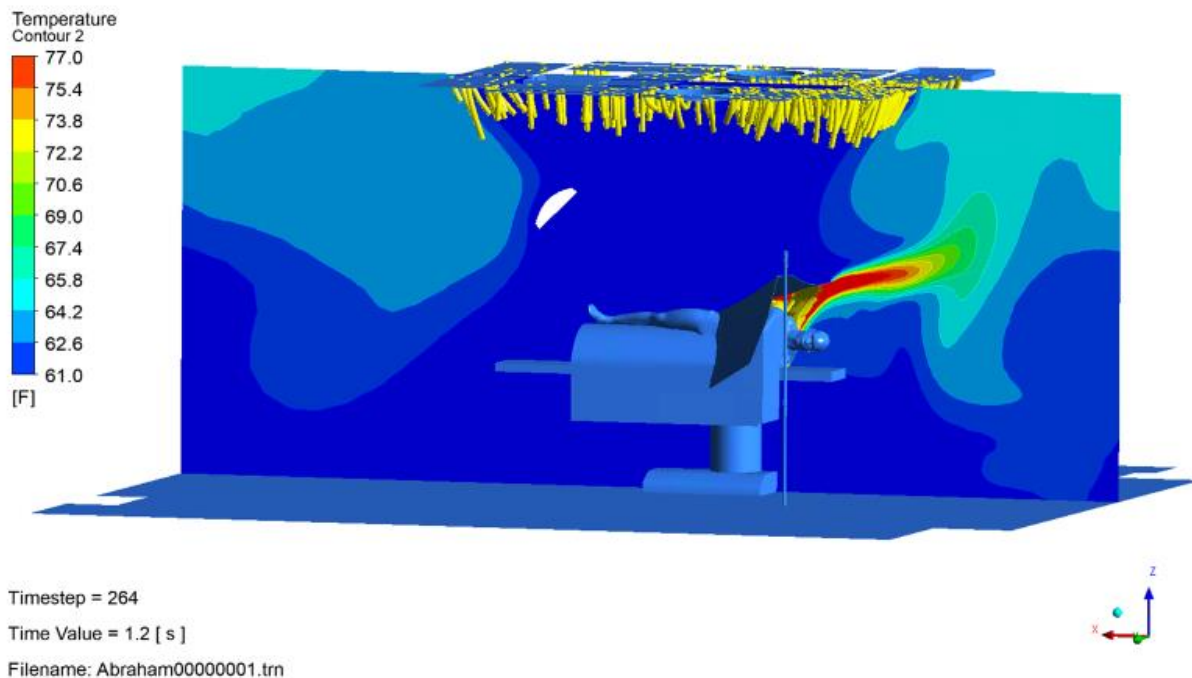


Figure 7 The temperature is contour plotted on a plane at $y = -3.85986$ (m), with the scale trimmed to 61.0 (°F) and 77 (°F) for the 2540_full.trn results. Yellow streamlines are added to show approximately the distance the inlet flows traveled in 1.2 (s).

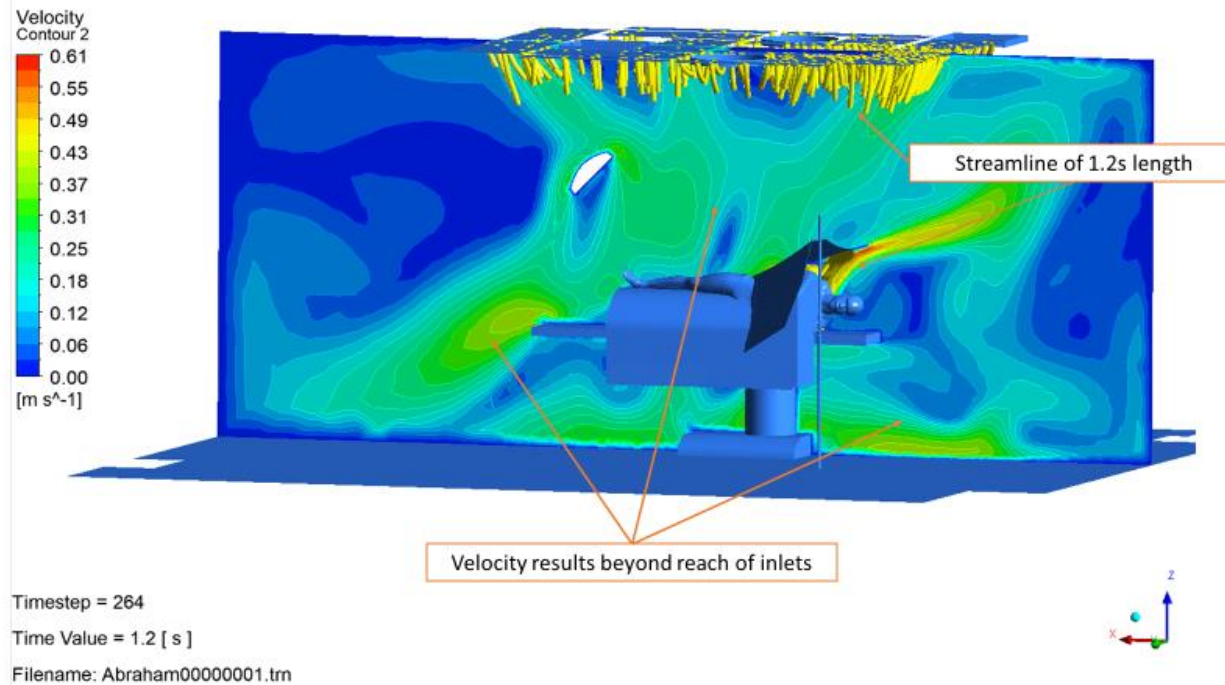


Figure 8 The velocity contour plotted on a plane at $y = -3.85986$ (m), for the Abraham00000001.trn results. Yellow streamlines are added to show approximately the distance the inlet flows traveled in 1.2 (s). Note the significant areas beyond the streamlines.

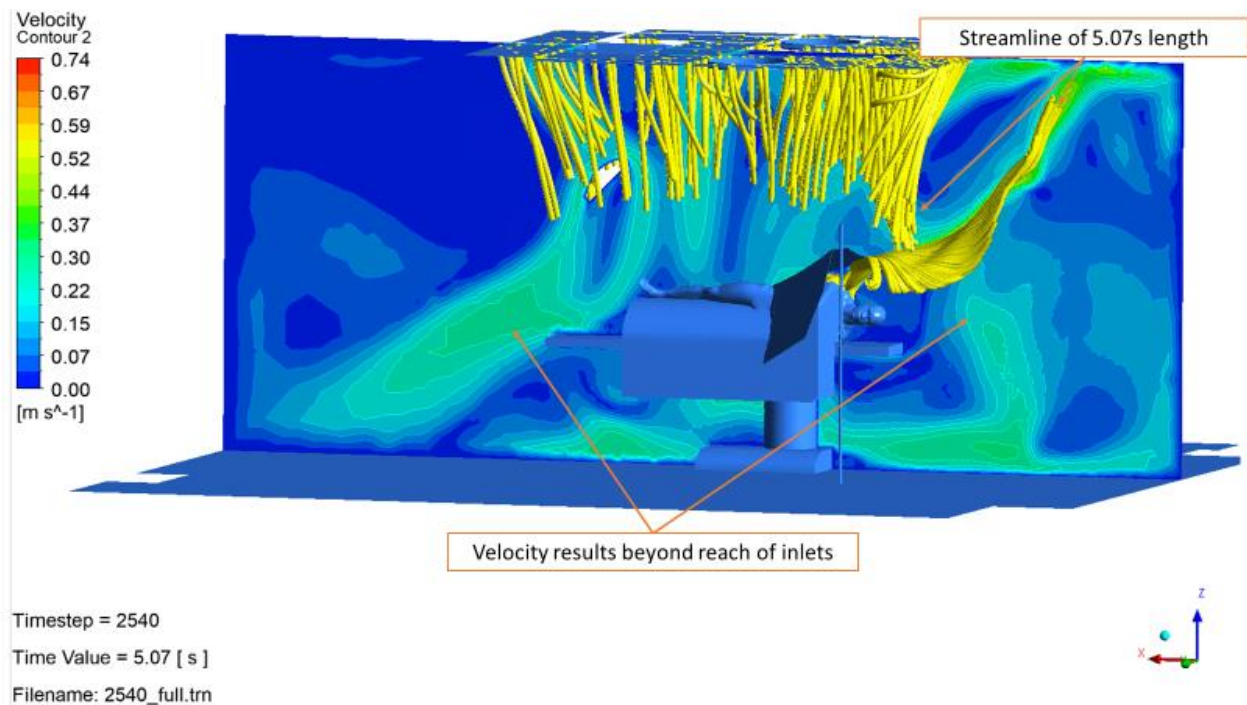


Figure 9 The velocity contour plotted on a plane at $y = -3.85986$ (m), for the 2540_full.trn results. Yellow streamlines are added to show approximately the distance the inlet flows traveled in 5.07 (s). Note the significant areas beyond the streamlines.

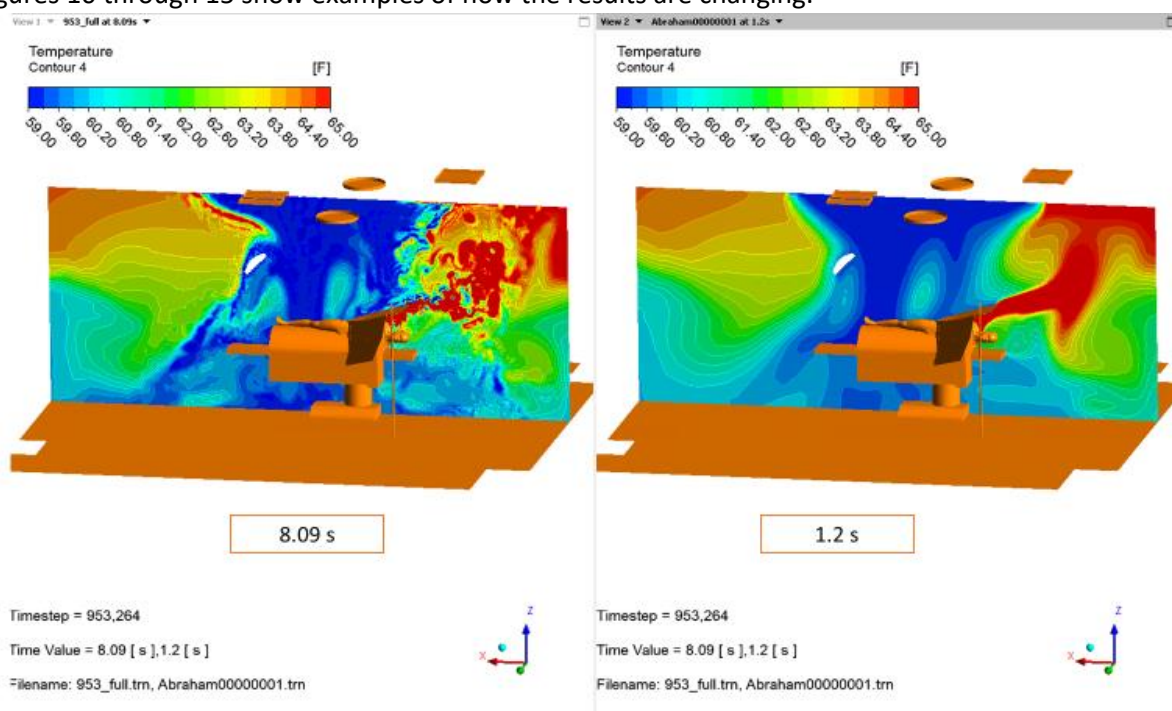
Results

The CFD solver will produce information at each of the elements/nodes at each timestep, these results are typically written to hard drives with some regular frequency. The intermediate result files are called trn files in CFX. Each trn result file contains the results at a specific time. The CFD post process is used to integrate the results, there are several different ways the results can be integrated, these include vector and contour plots and streamlines.

Changing results

The CFD results reported by Dr. Abraham only show the flow at the specific 1.2s (Abraham) and 5.07 (s) (2540_full) from unknown starting conditions, however if the transient models is run forward, the model results changes, as it would be expected given the short model times solved and the turbulent model choice. The model would have also been changing prior to the provided results at the specific timestep. Since the result change over time, it is not valid to use only a single specific timestep, since the results used would change dependent timestep was selected. It also means the steady state assumption cannot be used without error.

Figures 10 through 15 show examples of how the results are changing.



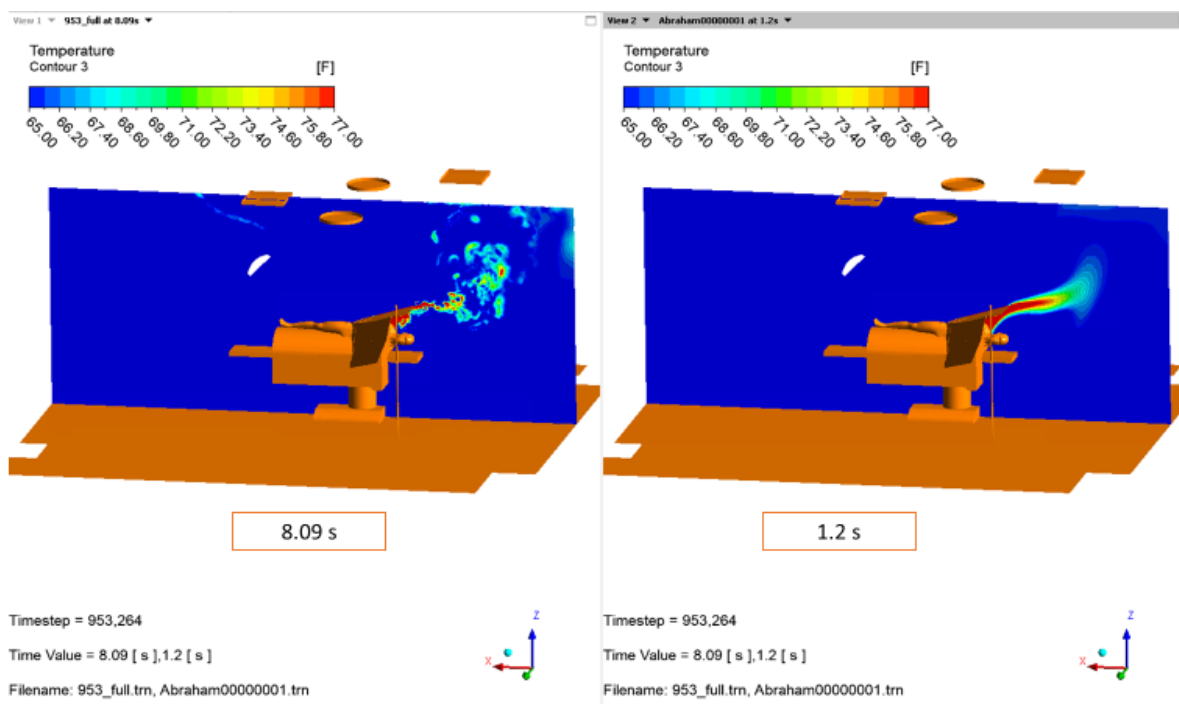


Figure 11 shows the difference in the temperature results once the Abraham00000001.trn model has been solved to 8.09 (s). Steady state requires that there is no change of any results with time, this is not the case. The temperature contours were limited to between 65.0 (°F) and 77 (°F) to help show the variation near the Bair Hugger Inlet

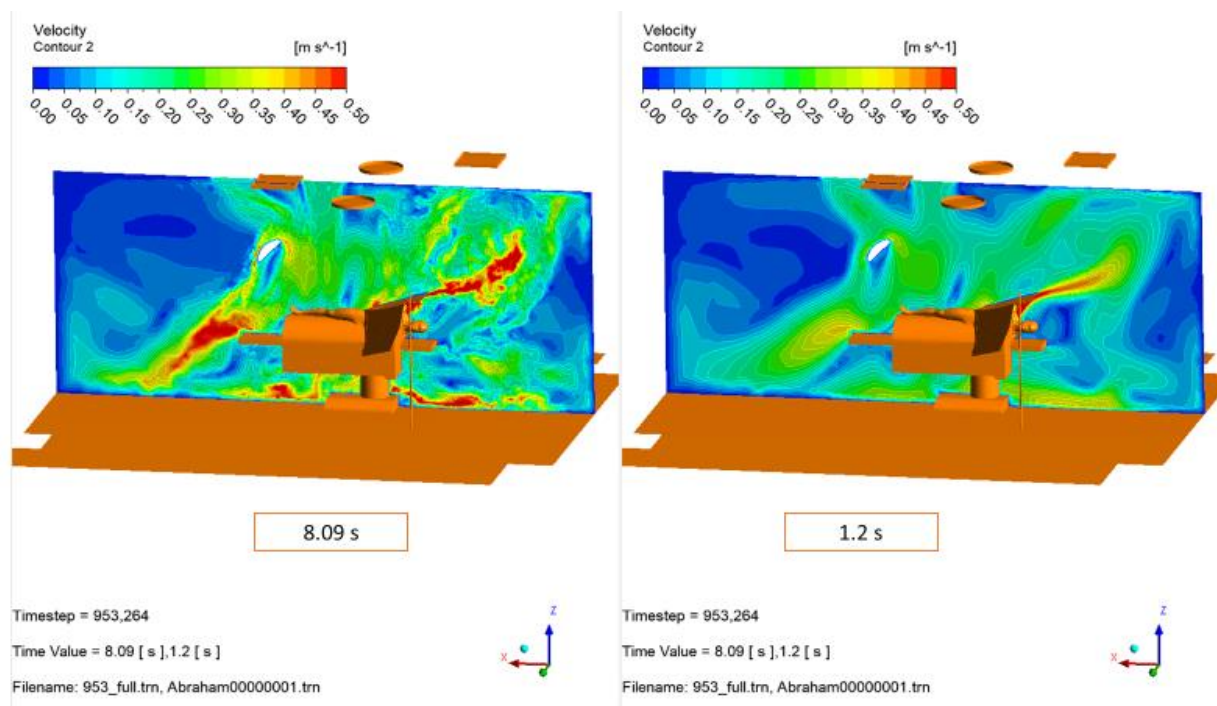


Figure 12 shows the difference in the velocity results once the Abraham00000001.trn model has been solved to 8.09 (s). Steady state requires that there is no change of any results with time

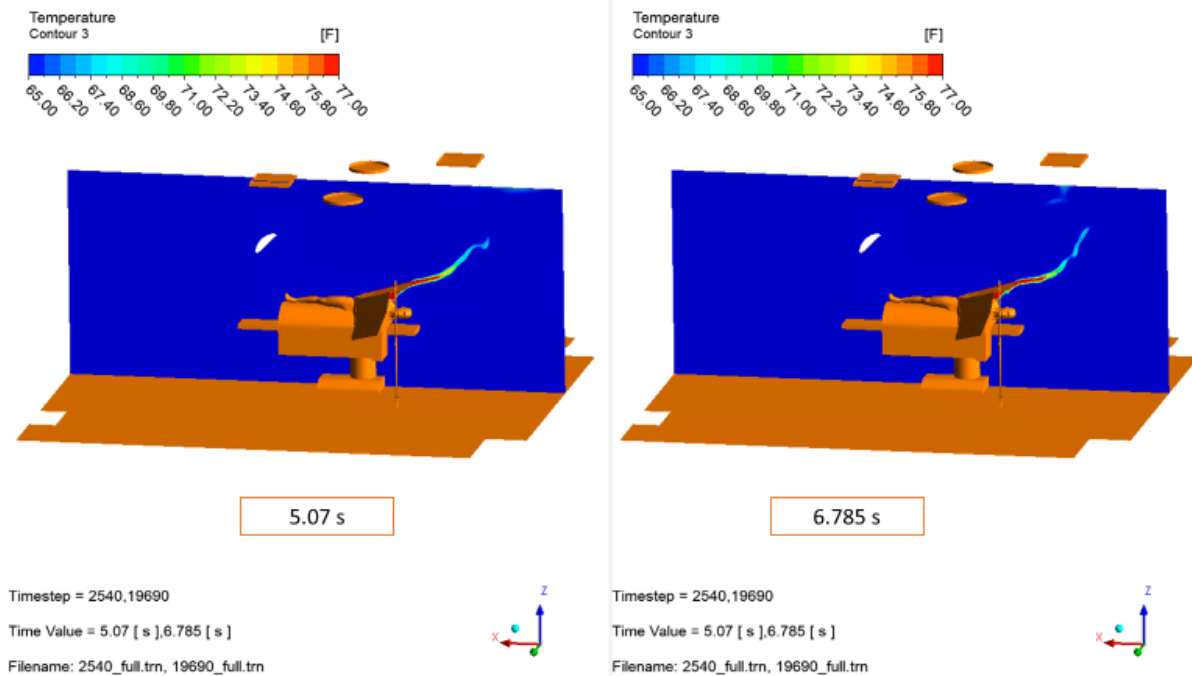


Figure 13 shows the difference in the velocity results once the 2540_full.trn model has been solved to 6.785 (s). Due to the scale, the differences are more subtle, a difference plot is shown in Figure 38 to highlight the differences.

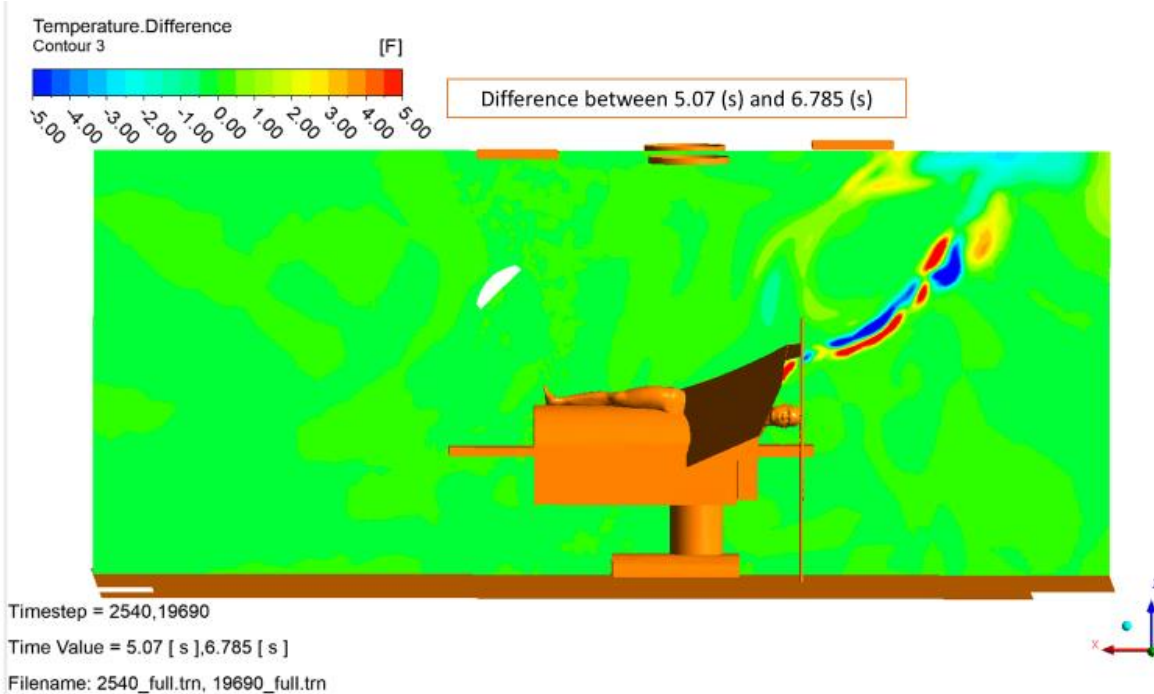


Figure 14 shows the difference in the velocity results once the 2540_full.trn model has been solved to 6.785 (s).

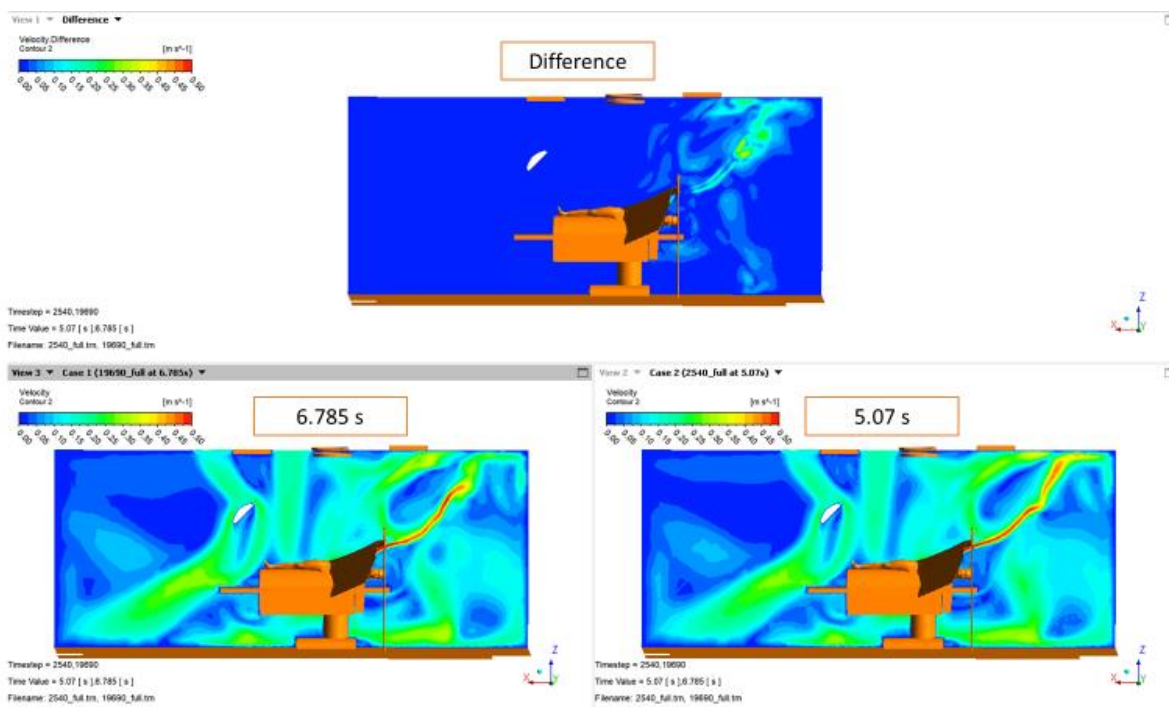


Figure 15 shows the difference in the velocity results once the 2540_full.trn model has been solved to 6.785 (s).

Turbulent Flow

When a fluid moves in a turbulent flow the fluid moves in an irregular, chaotic, unsteady manner. Eddies of different shapes and sizes are produced, these eddies will break down into smaller eddies which themselves can be transport by other larger eddies. Turbulence is by nature a transient phenomenon.

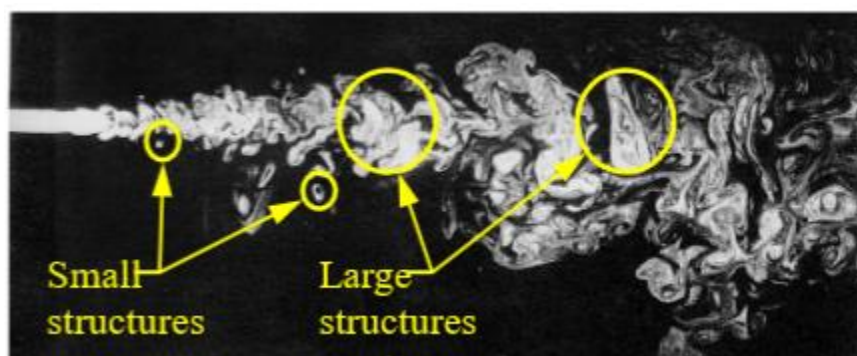


Figure 16 Picture of a turbulent jet. The turbulent structures will move downstream rotating and breakup in to smaller eddies.

WALE LES turbulence is a transient model

The WALE LES turbulence model Dr. Abraham has chosen to use can only be solve as a transient solution. For the model to work correctly the solution must resolve the changing details of the large turbulent structures like eddies as they change with time. The WALE LES model cannot be run steady state. *“alternative approaches of Large Eddy Simulation (LES) or Direct Numerical Simulation (DNS) can be adopted. With these methods, time dependent equations are solved for the turbulent motion”*¹

Turbulence at inlet

Dr. Abraham, states in his rebuttal to Elghobashi that the inlet has grate *“As airflow passes through the ceiling grill, small eddies and turbulence are created”* and that will produce turbulence, however he does not include any turbulence at either of his inlets (Figures 17 and 18).

Table 7. Boundary Physics for Abraham00000001

Domain	Boundaries
FluidRegion	Boundary - Inlet
Type	INLET
Location	Inlet Lights
	Settings
Flow Direction	Normal to Boundary Condition
Flow Regime	Subsonic
Heat Transfer	Static Temperature
Static Temperature	5.9000e+01 [F]
Mass And Momentum	Mass Flow Rate
Mass Flow Rate	1.3870e+00 [kg s ⁻¹]
Mass Flow Rate	As Specified

Figure 17 Inlet boundary definition for Abraham00000001.trn

Table 4. Boundary Physics for 2540_full

Domain	Boundaries
FluidRegion	Boundary - Inlet
Type	INLET
Location	Inlet Lights
	Settings
Flow Direction	Normal to Boundary Condition
Flow Regime	Subsonic
Heat Transfer	Static Temperature
Static Temperature	5.9000e+01 [F]
Mass And Momentum	Mass Flow Rate
Mass Flow Rate	1.3870e+00 [kg s ⁻¹]
Mass Flow Rate Area	As Specified

Figure 18 Inlet boundary definition for 2540_full.trn

Streamlines

For streamline to accurately capture the motion of the flow the model velocity field must not change.

¹ 4.1.11.2 Introduction to LES, CFX-Solver Modeling Guide, Ansys Help.

Streamline require a steady state flow conditions to be accurate.

Dr. Abraham used a transient model to predict the velocity fields. The velocity solution that the streamline uses to calculate their paths changes with time making the steady state assumption incorrect.

Additionally, Dr. Abraham used a transient turbulence model to predict the velocity fields, the model cannot be run steady state as it need to change the velocity solution over time to explicitly model turbulence correctly. Steady state streamlines are inaccurate when used with a changing velocity field like one produced by the LES model.

Both errors together and independently cause the streamlines path to change depending on which timestep is choose. For the assumption to be valid the choice of timestep should not change the streamline path. Figures 19 through 27 show examples of how a streamline path will change depending on which transient result is used with the steady state streamlines. The predicted path also changes resulting in very unphysical prediction, like particle appearing and disappearing around the model a completely unphysical manor.

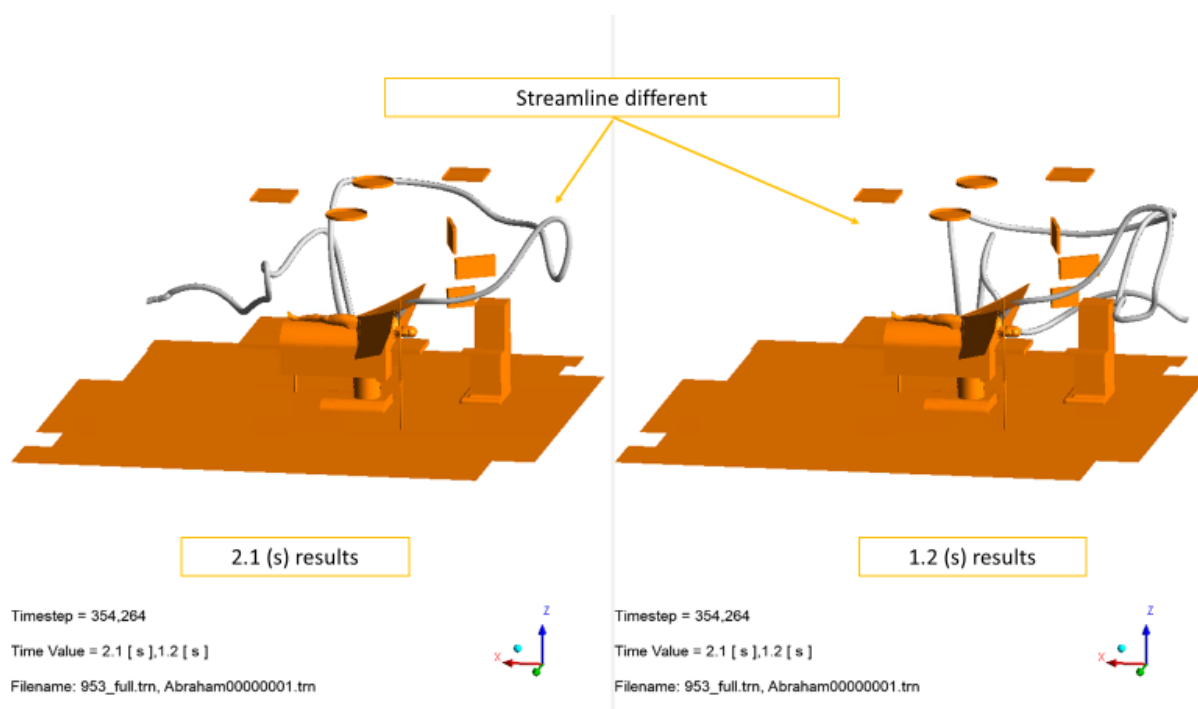


Figure 19 shows the predicted path of a streamline coming from the Bair Hugger Inlet for Abraham00000001.trn model for both 2.1 (s) on the left and the 1.2 (s) report on the right. The difference streamline paths is due the changes to the underlying velocity solution.

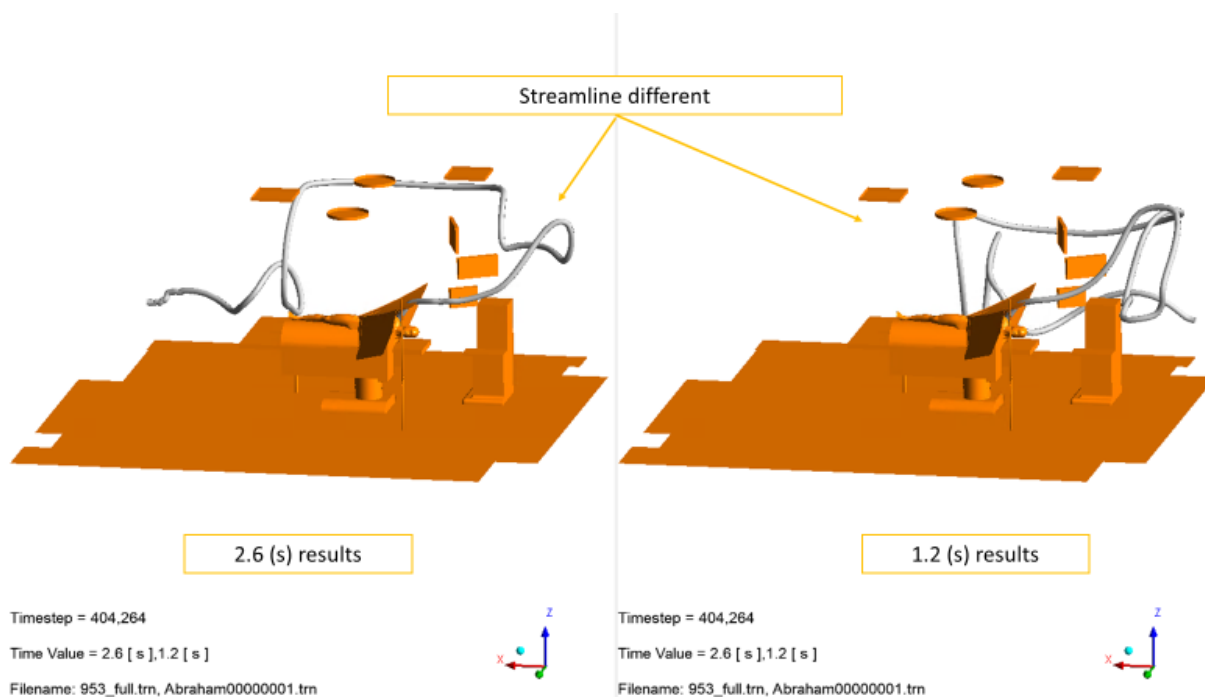


Figure 20 shows the predicted path of a streamline coming from the Bair Hugger Inlet for Abraham00000001.trn model for both 2.6 (s) on the left and the 1.2 (s) report on the right. The difference streamline paths is due the changes to the underlying velocity solution.

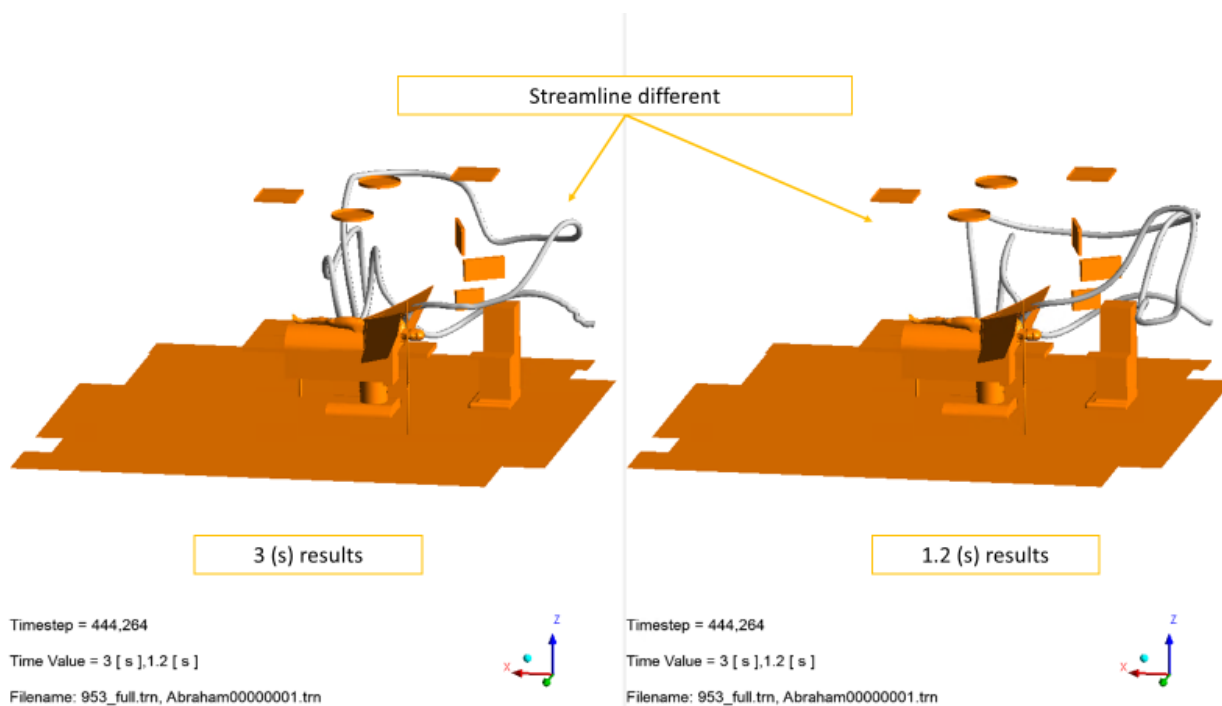


Figure 21 shows the predicted path of a streamline coming from the Bair Hugger Inlet for Abraham00000001.trn model for both 3 (s) on the left and the 1.2 (s) report on the right. The difference streamline paths is due the changes to the underlying velocity solution.

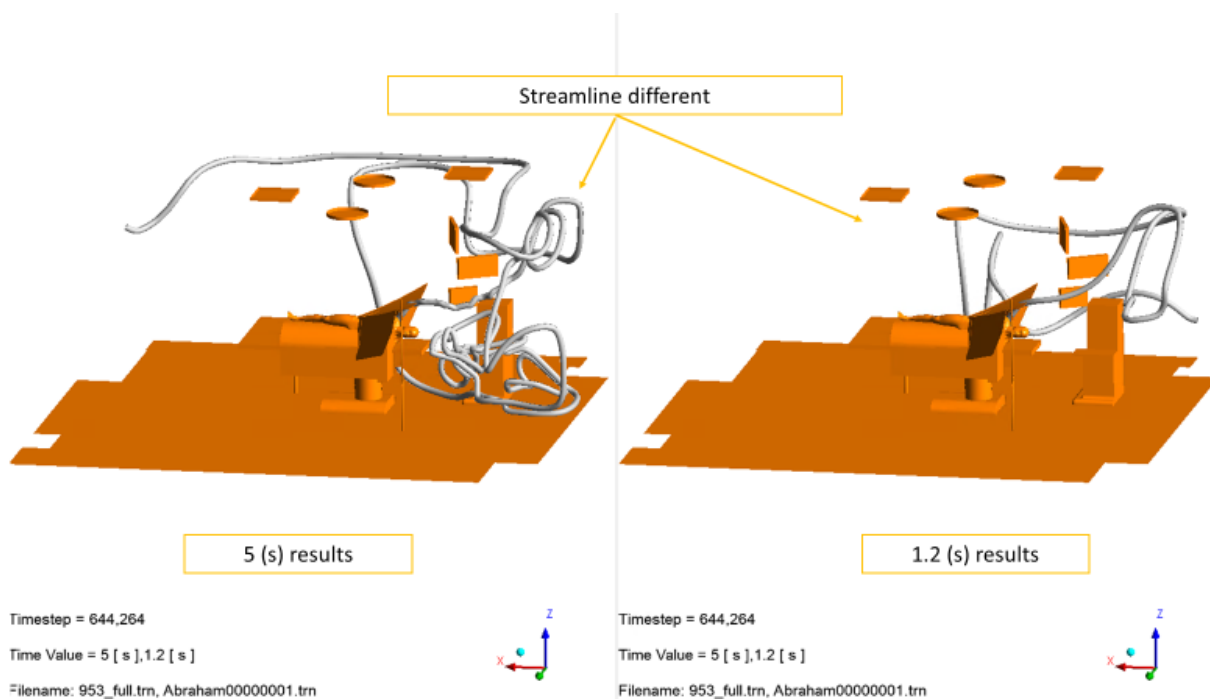


Figure 22 shows the predicted path of a streamline coming from the Bair Hugger Inlet for Abraham00000001.trn model for both 5 (s) on the left and the 1.2 (s) report on the right. The difference streamline paths is due the changes to the underlying velocity solution.

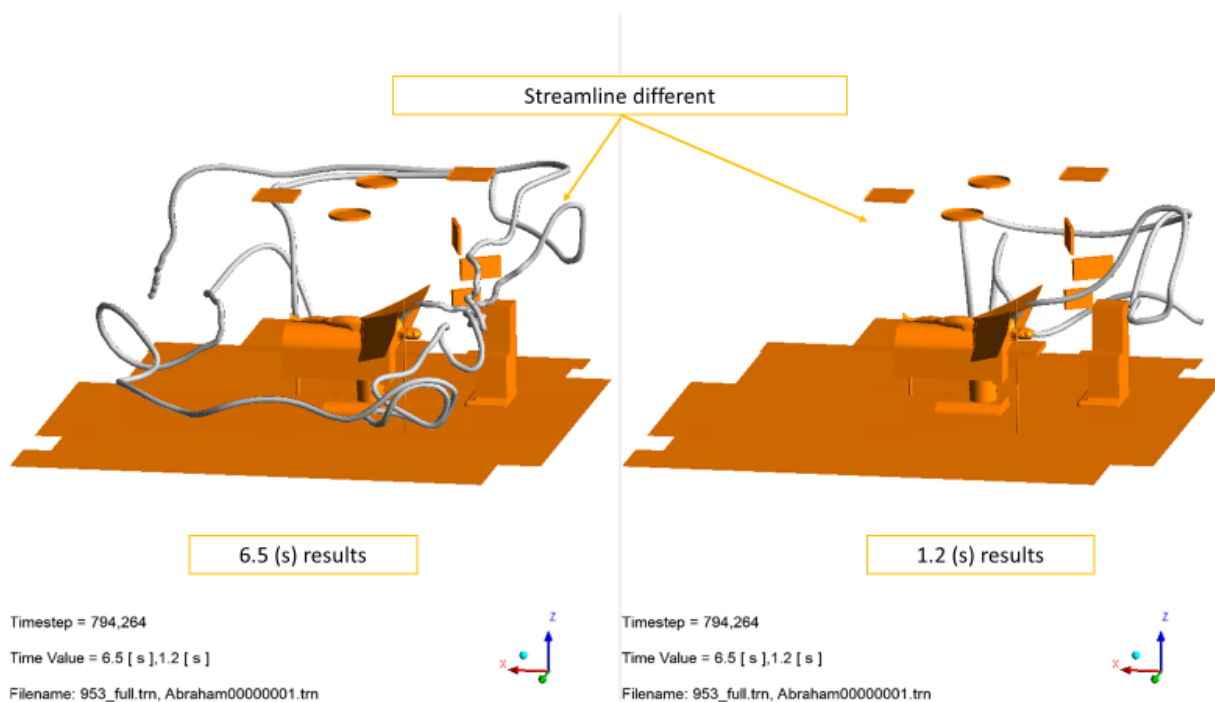


Figure 23 shows the predicted path of a streamline coming from the Bair Hugger Inlet for Abraham00000001.trn model for both 6.5 (s) on the left and the 1.2 (s) report on the right. The difference streamline paths is due the changes to the underlying velocity solution.

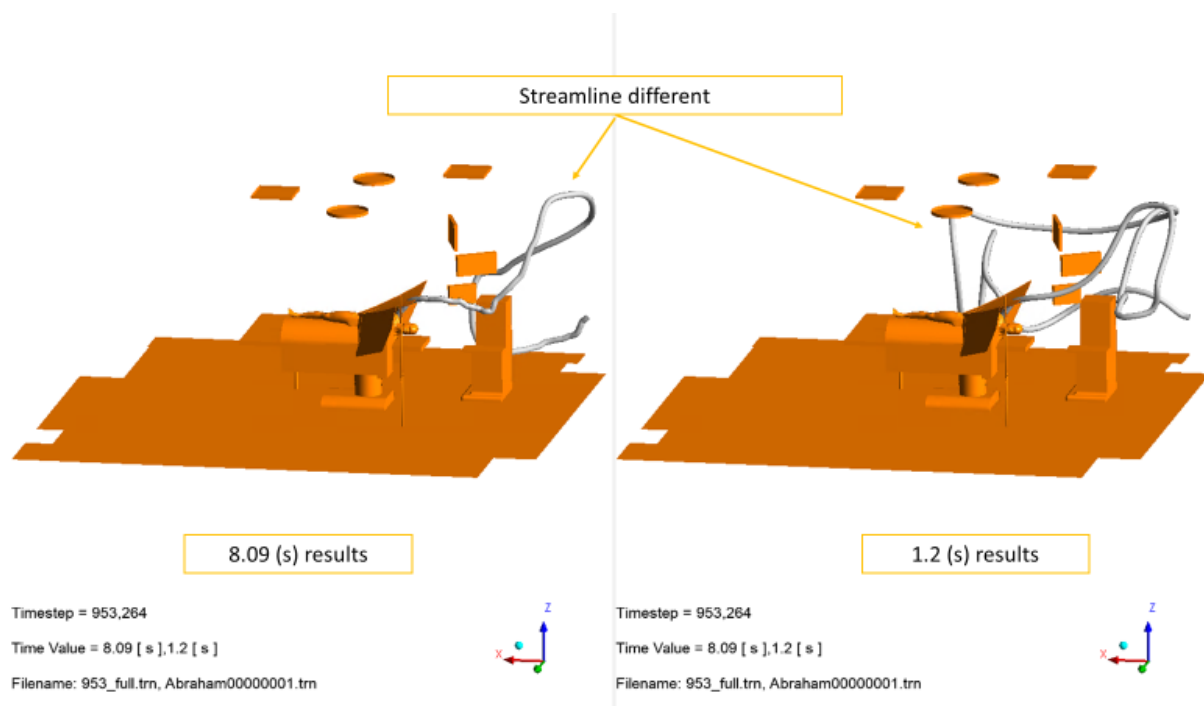


Figure 24 shows the predicted path of a streamline coming from the Bair Hugger Inlet for Abraham00000001.trn model for both 8.09 (s) on the left and the 1.2 (s) report on the right. The difference streamline paths is due the changes to the underlying velocity solution.

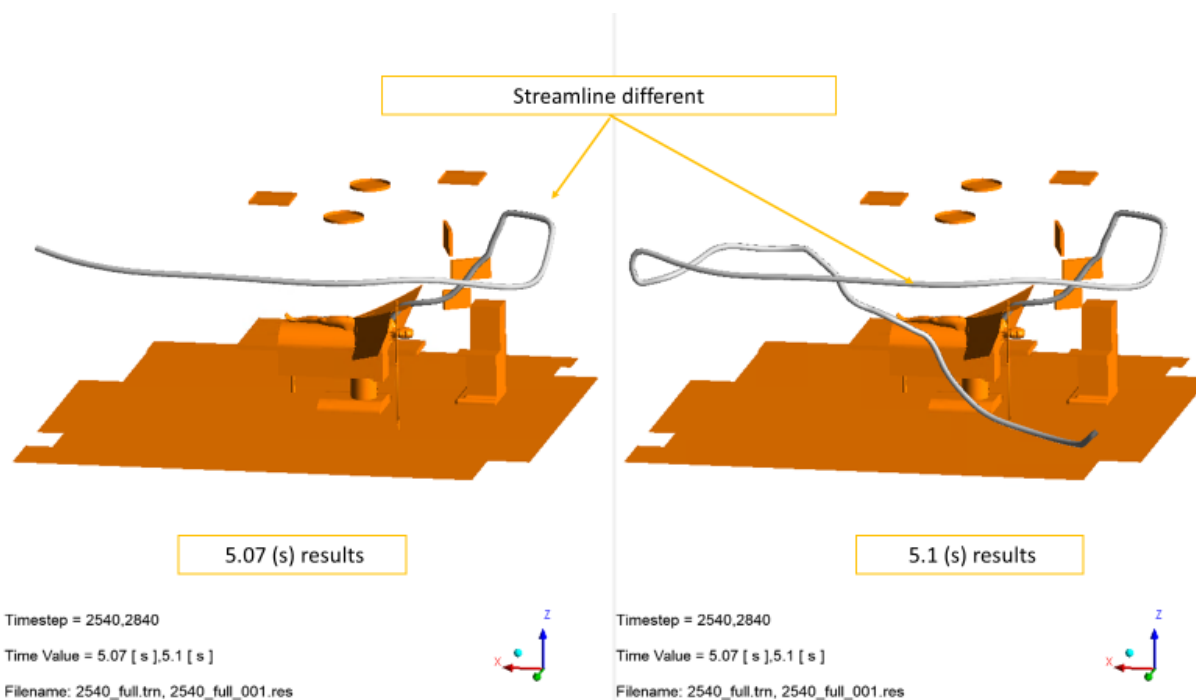


Figure 25 shows the predicted path of a streamline coming from the Bair Hugger Inlet for 2540_full.trn model for both 5.07 (s) on the left and the 5.1 (s) report on the right. The difference streamline paths is due the changes to the underlying velocity solution.

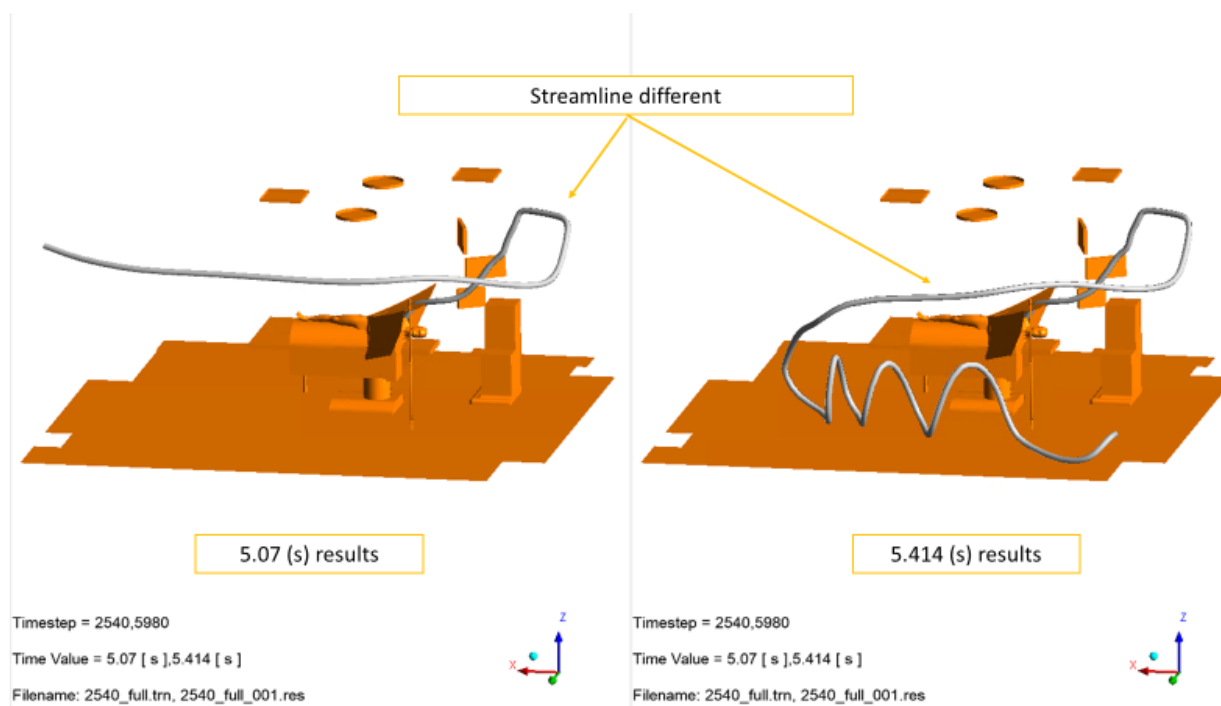


Figure 26 shows the predicted path of a streamline coming from the Bair Hugger Inlet for 2540_full.trn model for both 5.07 (s) on the left and the 5.414 (s) report on the right. The difference streamline paths is due the changes to the underlying velocity solution.

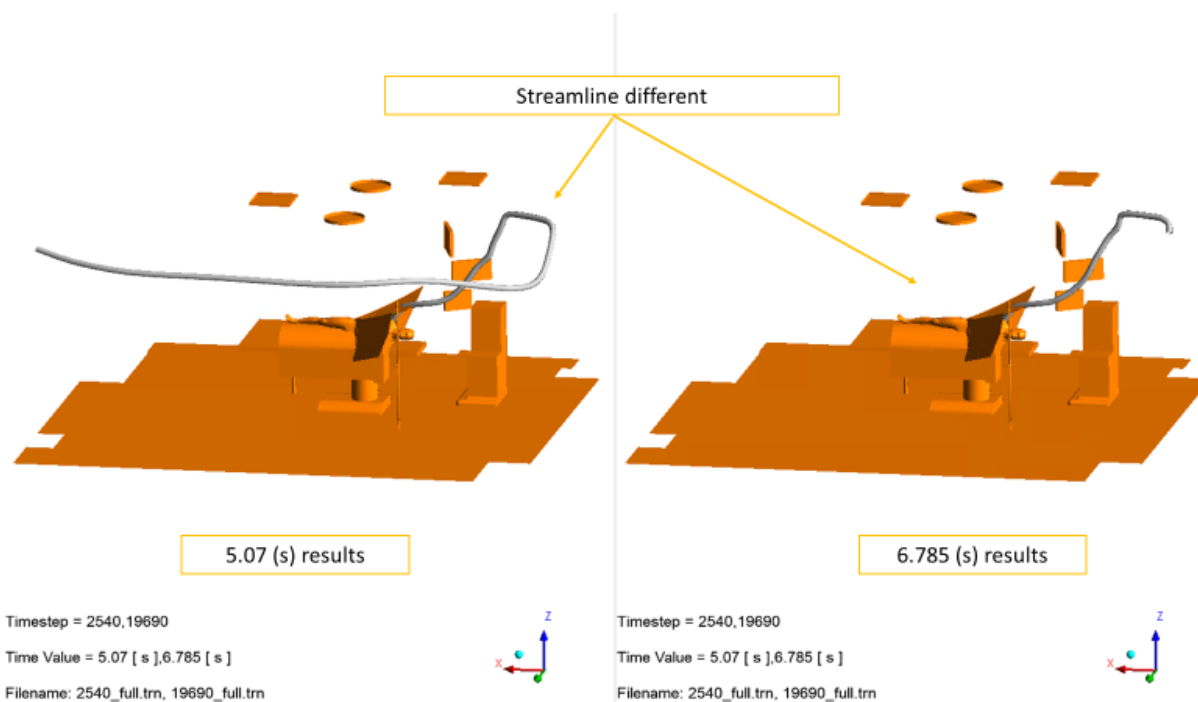


Figure 27 shows the predicted path of a streamline coming from the Bair Hugger Inlet for 2540_full.trn model for both 5.07 (s) on the left and the 6.785 (s) report on the right. The difference streamline paths is due the changes to the underlying velocity solution.

Streamlines do not capture settling (buoyancy) or slip

As a particle moves through a fluid, a number of different forces act on them, these forces include slip and will change the particles trajectory compared to what a streamline would predict. Both slip and buoyancy are known to effect particles, in fact, a lot of separation technology (cyclones and separators) are designed to use these forces in their designs. Streamlines do not include either forces.

Streamlines do not capture Turbulence Dispersion

The unsteady eddies in turbulent flow will cause particles to spread away from an average particle path line. This turbulent dispersion will result in particles released from the same point to take potentially very different paths depending on when they are released. Streamline do not capture the physical effect, to do so correctly would require modeling the particles as transient particles, which ANSYS CFX has the capability to do.

Mesh

In a CFD model the geometry (volume) that the air moves through is split into a discrete number of mesh cells. It is important that mesh contains enough nodes/elements, so the results are independent of the mesh used. The elements of the mesh also need to be within quality limitation or else the solver can have issues solving and/or give incorrect results.

Unacceptable mesh quality

Dr. Abraham has a number of his mesh elements that are not in the acceptable range of mesh quality as defined by ANSYS. Figure 28 through 31. Poor quality mesh elements are known to cause convergence issues and give incorrect answers (Figures 32 and 33).

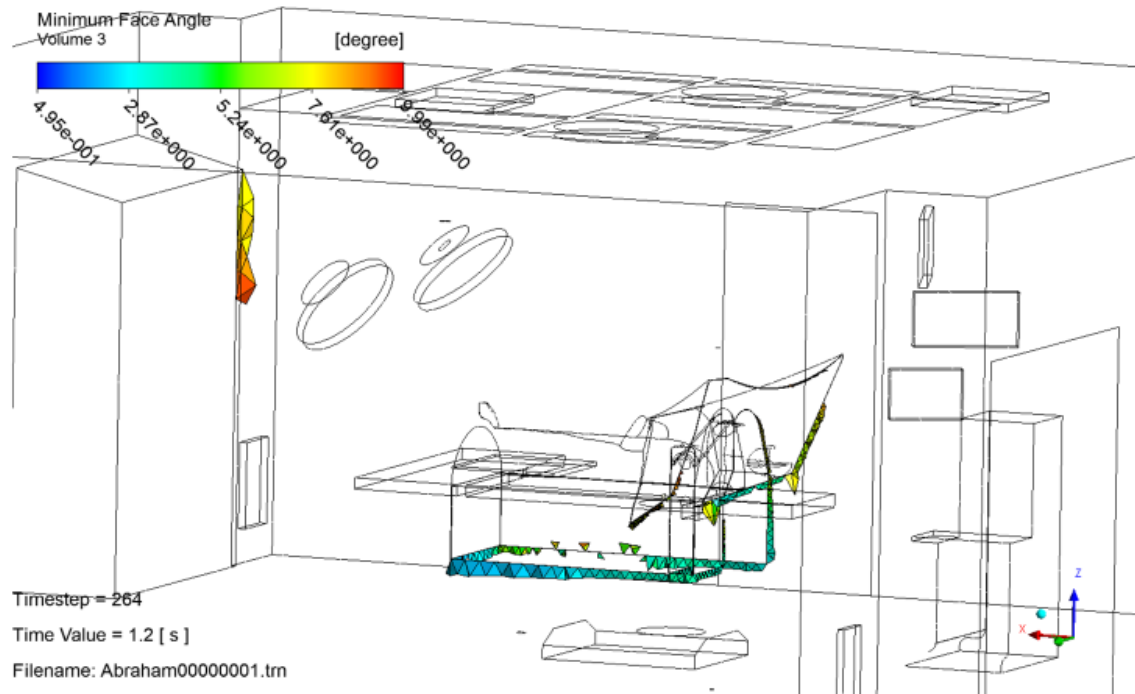


Figure 28 Poor Mesh quality Abraham00000001.trn Minimum Face Angle

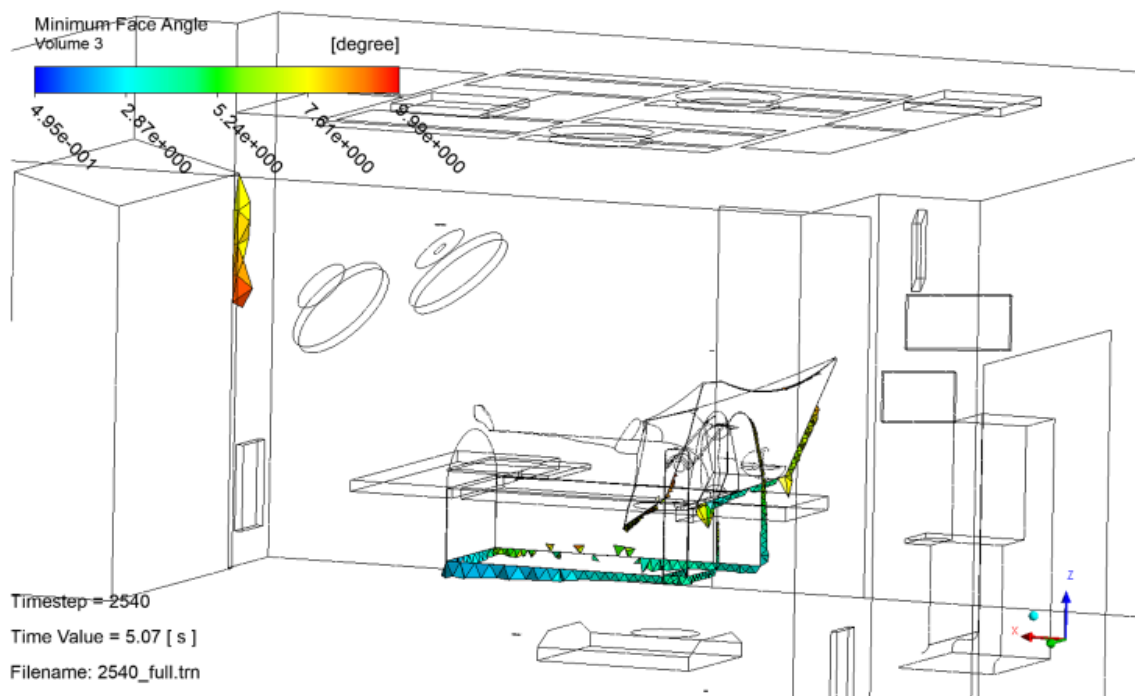


Figure 29 Poor Mesh quality 2540_full.trn Minimum Face Angle

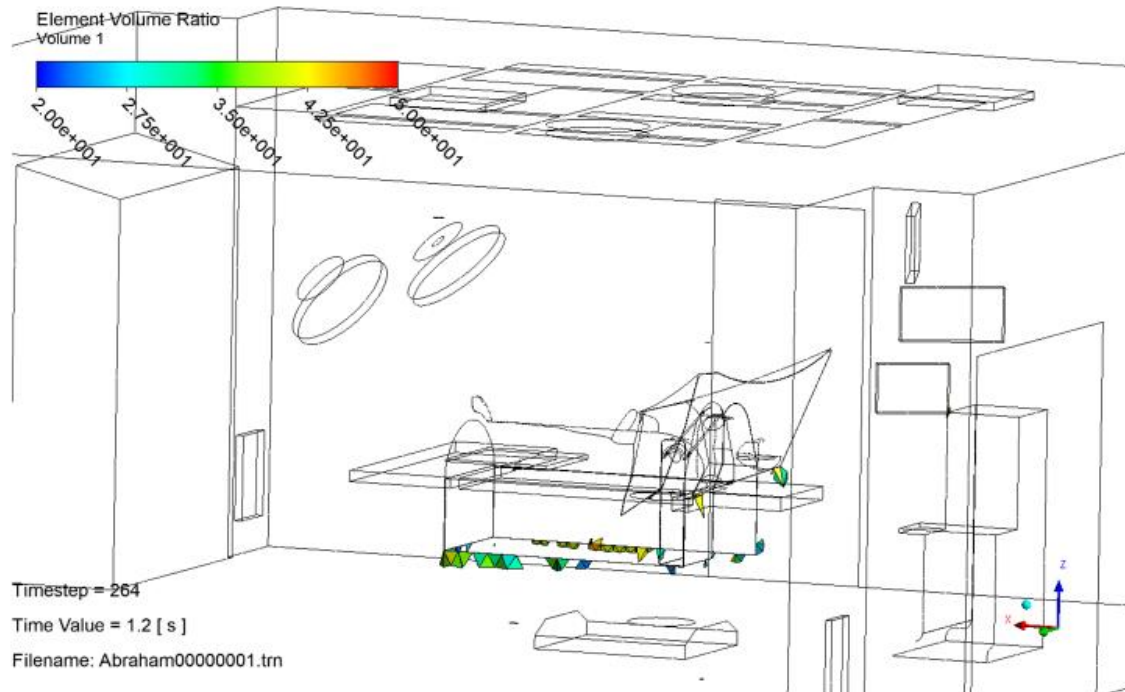


Figure 30 Poor Mesh quality Abraham00000001.trn Element Volume Ratio

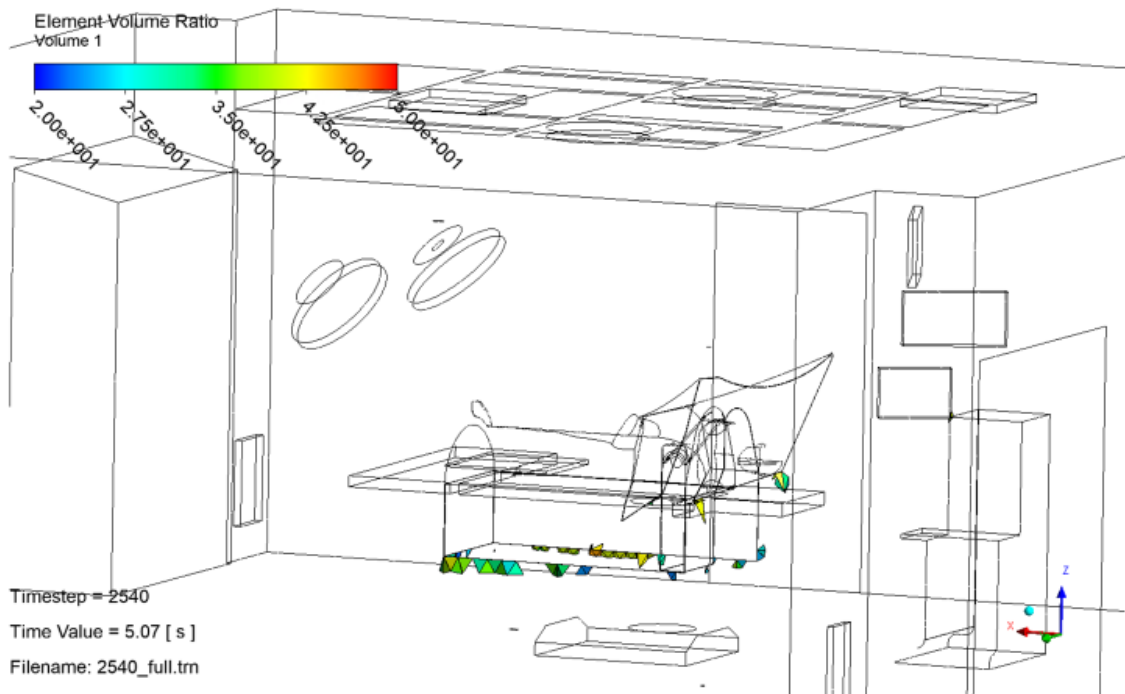


Figure 31 Poor Mesh quality 2540_full.trn Element Volume Ratio

19.3.2.1. Mesh Orthogonality

The concept of mesh orthogonality relates to how close the angles between adjacent element faces or adjacent element edges are to some optimum angle (for example, 90° for quadrilateral-faced elements and 120° for triangular-faced elements). The most relevant measure of mean orthogonality for the CFX Solver is illustrated below. It involves the angle between the vector that joins two mesh (or control volume) nodes ij and the normal vector for each integration point surface ij associated with that edge. Significant orthogonality and non-orthogonality are illustrated in the figure, respectively.



The orthogonality angle, three related measures, and acceptable ranges are tabulated below with other measures that are available through the CFX-Post postprocessor and ANSYS CFX Solver tools. Values outside of the suggested acceptable range will increase both round-off and the amplification of discretization error. Poor convergence and divergence can be expected under these conditions.

Orthogonality Measure	Acceptable Range	Description and Notes
Orthogonality Angle	$\approx 90^\circ$	Area weighted average of $\cos(\theta) = \cos(\theta_{ij})$ for all integration point surfaces of a control volume. + Large values indicate good orthogonality. + One of the best indicators of how and where poor orthogonality will adversely affect general solution accuracy and robustness.
Orthogonality Factor	≈ 1	Area weighted average of all integration point surface scalar products of unit n and n_{ij} vectors that is $n \cdot n_{ij}$ associated with each control volume. + Large values indicate good orthogonality. + One of the best indicators of how and where poor orthogonality will adversely affect general solution accuracy and robustness.
Orthogonality Angle Minimum	$\approx 10^\circ$	Minimum of $\cos(\theta) = \cos(\theta_{ij})$ for all integration point surfaces of a control volume. + Smaller the orthogonality angle, the adverse effects are likely to be less globally significant.
Orthogonality Factor Minimum	≈ 0.2	Minimum of all integration point surface scalar products of unit n and n_{ij} vectors that is $n \cdot n_{ij}$ associated with each control volume. + Smaller the orthogonality angle, the adverse effects are likely to be less globally significant.
Minimum Maximum Face Angle (CFOFace)	$\approx 10^\circ$ or $\approx 120^\circ$	Minimum/maximum angle between edges of each face that touches a node. + Usefulness of this orthogonality measure is limited by its two-dimensional nature. + Acceptable non-orthogonality values do not ensure acceptable orthogonality. For example, a balanced distribution can have minimum angles of 90°.

Figure 32 Mesh quality recommendations Mesh Aspect Ratio²

19.3.2.3. Mesh Aspect Ratio

The concept of the mesh aspect ratio relates to the degree that mesh elements are stretched. The most relevant measure of aspect ratio for the CFX Solver is illustrated below. It involves the ratio of the maximum to minimum integration point surface areas in all elements. Nodeal (that is, control volume) values are calculated as the maximum of all element aspect ratios that are adjacent to the node.



The area based measure is tabulated below along with another measure that is available through the CFX-Post postprocessor. Values outside of the suggested acceptable range will lead to round-off errors and associated difficulties converging the discretized equations.

Mesh Aspect Ratio Measure	Acceptable Range	Description and Notes
Aspect Ratio	$\approx 100R$	Largest ratio of maximum to minimum integration point surface areas for all elements adjacent to a node.
Edge Length Ratio (CFDPost)	≈ 100	Largest ratio of maximum to minimum integration edge lengths for all edges of element faces that touch a node.

^{1R} The acceptable range for both measurements is less than 1000 if running double precision.

Figure 33 Mesh quality recommendations³

Mesh dependence of solution

Dr. Abraham does not have an adequately refined mesh. If Dr. Abraham was to run his model on a more refined mesh he would get a different result. It is standard industry practice to establish mesh independence of your model results.

Based on the best practice guidelines for LES modelling using ANSYS CFX by F.R. Menter⁴ LES models require a fine enough mesh that can capture the large eddies. The $l_{S_{crit}}$ is an estimate of the number of nodes that shall be available to capture high resolution turbulent features for any LES simulation. It is calculated from,

$$l_{S_{crit}} = \frac{l_t}{l_{mesh}} \quad (1)$$

² ANSYS Help

³ ANSYS Help

⁴ Best Practice: Scale-Resolving Simulations in ANSYS CFD, Version 2.00, F.R. Menter

where l_t is the turbulent length scale and l_{mesh} is representing the mesh length scale.

The mesh length scale calculated from,

$$l_{mesh} = \sqrt[3]{V} \quad (2)$$

where V is the mesh sector volume for a node.

The turbulent length scale l_t is calculated from,

$$l_t = \frac{k^{3/2}}{\varepsilon} \quad (3)$$

where k is the resolved kinetic turbulent energy which is from,

$$k = \frac{1}{2}(\overline{u'^2} + \overline{v'^2} + \overline{w'^2}) \quad (4)$$

where $\overline{u'^2}$, $\overline{v'^2}$ and $\overline{w'^2}$ are the statistical Reynolds stresses, ε is the turbulent eddy dissipation which can be calculated using the following relationship

$$\varepsilon = \rho C_\mu \frac{k^2}{\mu_t} \quad (5)$$

where C_μ is dimensionless constant of 0.09, μ_t is the eddy viscosity.

Figures 35 and 37 show the LES mesh criteria for the Abraham00000001.trn and 2540_full.trn has significant areas with less than 5 elements and even areas with less than 1, Figures 36 and 38. The mesh resolution is too coarse to capture the required turbulent features and with refinement would produce different results. It is recommended that a minimum of 5-10 elements ratio to the turbulent integral length scale to capture the required details for any LES type turbulence modelling (Figure 34). Based on the conclusion captured by F. R. Menter· Y. Egorov⁵, *"In contrast, LES and DES models can return incorrect results and potentially numerical instabilities if the numerical grid is too coarse (insufficient for LES) or the time-step is too large (substantially larger than CFL ~1)."*, thus LES models can return significant error and the wrong results if the numerical mesh is too coarse.

⁵ The Scale-Adaptive Simulation Method for Unsteady Turbulent Flow Predictions. Part 1: Theory and Model Description F. R. Menter· Y. Egorov

4.2.3. Meshing Requirements

In order to generalize the concepts discussed for the mixing layer example (Figure 23), we introduce the terminology of a Separating Shear Layer (SSL). It refers to the shear layer that starts

33

at the point of separation from the body and moves into a free shear flow (we are not considering small separation bubbles embedded within the boundary layer). In Figure 23 this would be the mixing layer forming downstream of the plate. In other flows it can be a separating boundary layer from a corner. In the case of locally unstable flows, the Δ_{\max} spacing should be sufficiently small to allow resolution of the initial flow instability of the SSL. The main quantity of relevance is the ratio of RANS to grid length scale:

$$R_L = \frac{\Delta_{\max}}{L_t^{RANS}}; \quad L_t^{RANS} = \left(\frac{k^{3/2}}{\varepsilon} \right)^{RANS} = \left(\frac{k^{1/2}}{C_\mu \omega} \right)^{RANS}$$

It is important to emphasize that this quantity should be evaluated based on a precursor RANS solution. This implies that such a solution exists and is meaningful. If the precursor solution is not available, then one can estimate the ratio based on the thickness of SSL. For equilibrium mixing layers, the following ratio is approximately correct:

$$L_t^{RANS} = 0.7 \cdot \delta^{mixing}$$

where δ^{mixing} is the thickness of the mixing layer. The value of R_L should be:

$$R_L \leq 0.2 - 0.1$$

Figure 34 Best Practice: Scale-Resolving Simulations in ANSYS CFD, Version 2.00, by F.R. Menter, page 34

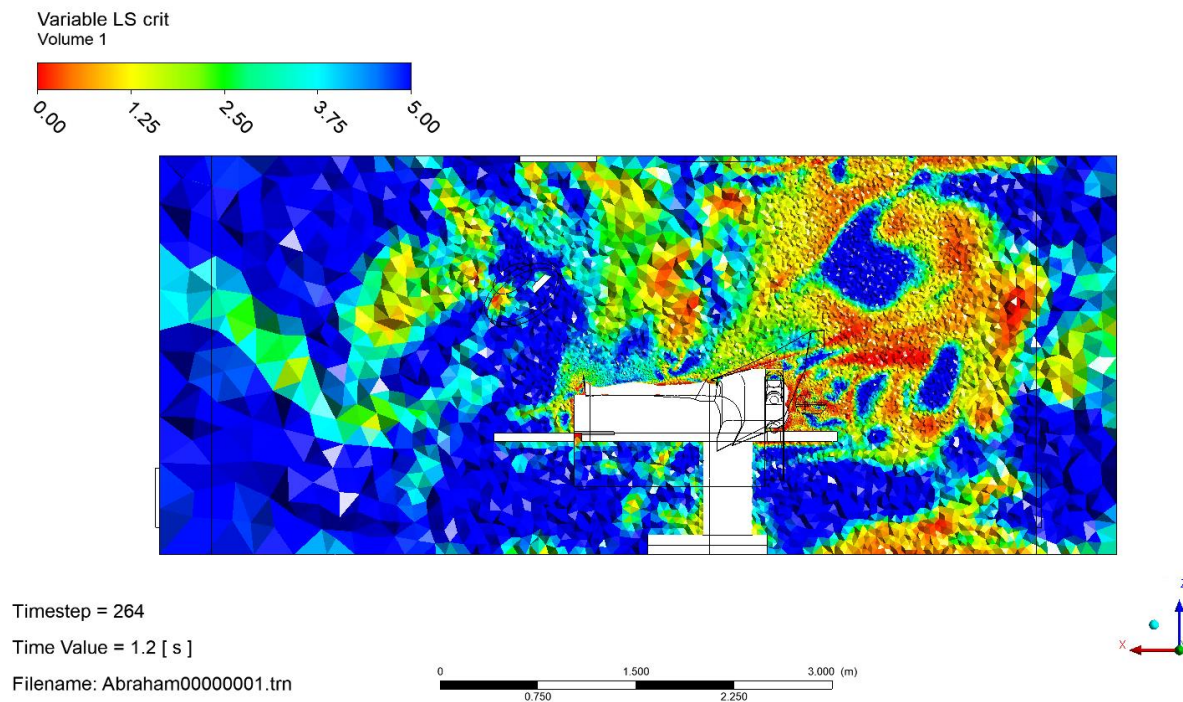


Figure 35 Mesh Criteria Abraham00000001.trn

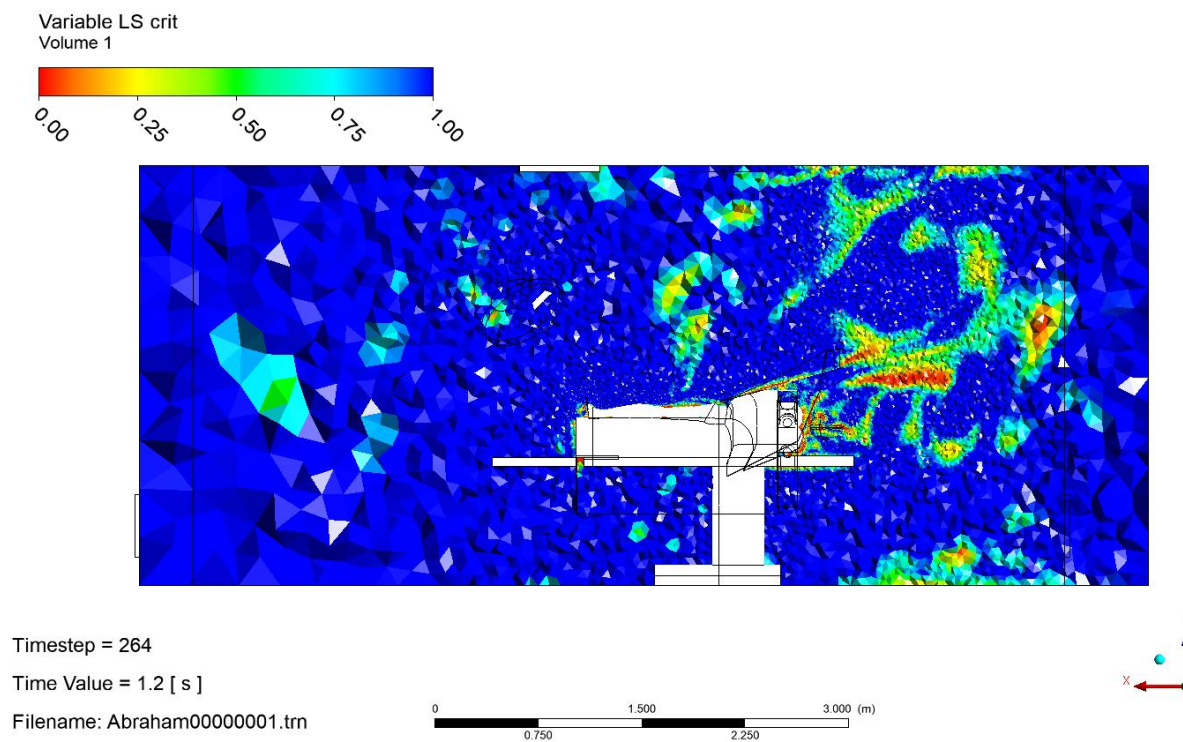


Figure 36 Mesh Criteria Abraham00000001.trn

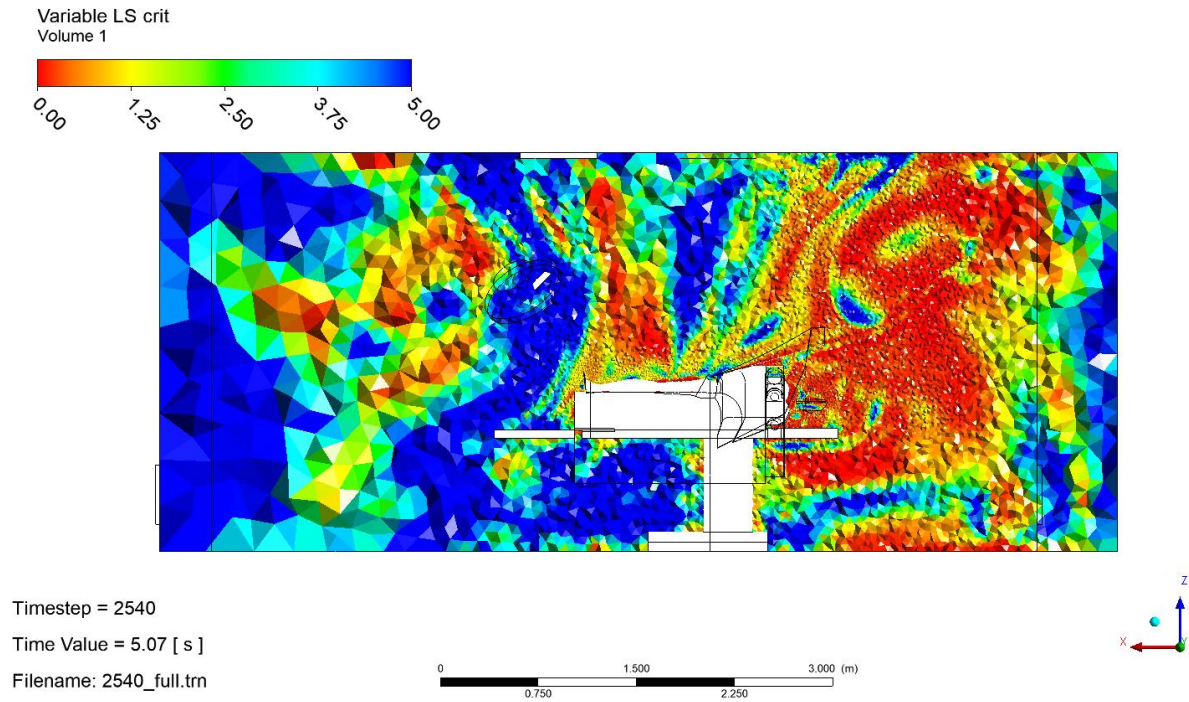


Figure 37 Mesh Criteria 2540_full.trn

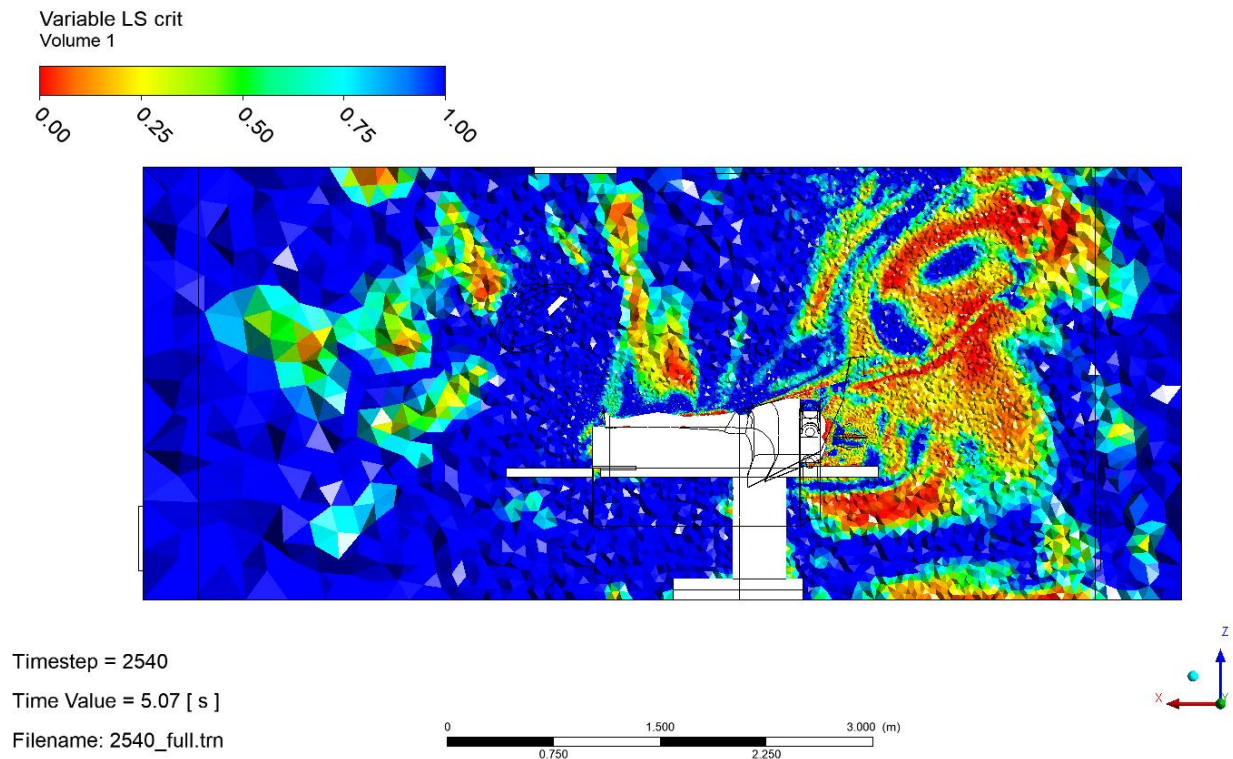
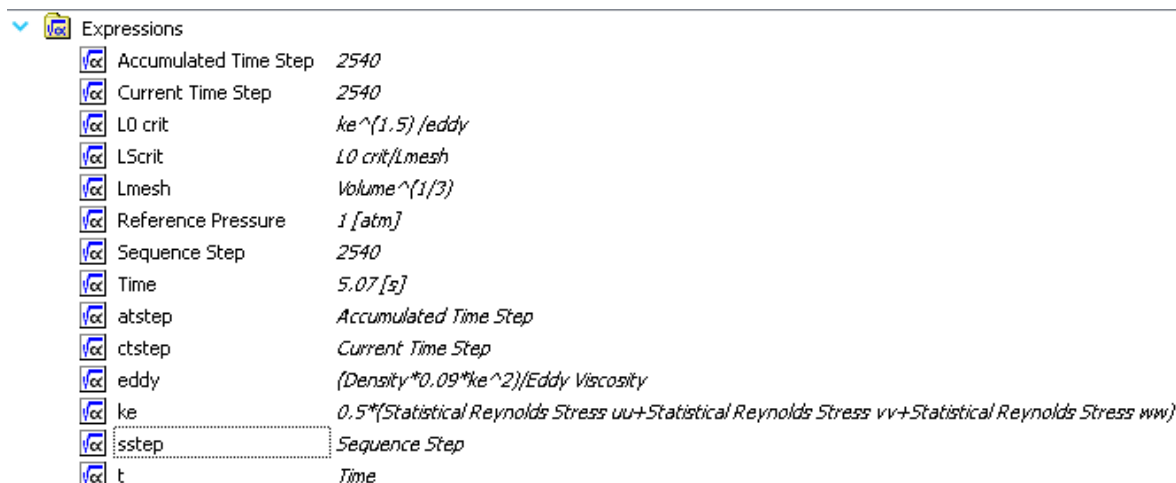
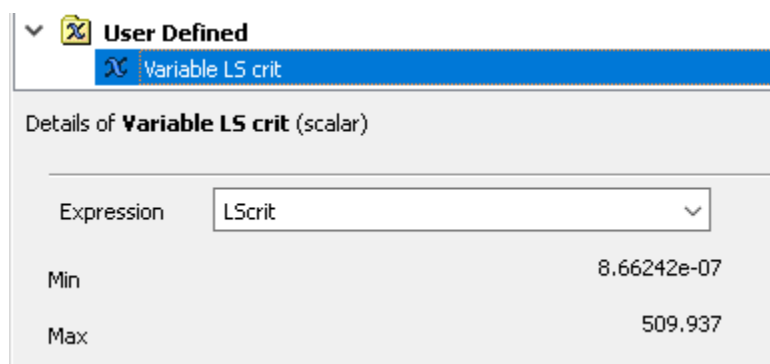


Figure 38 Mesh Criteria 2540_full.trn



Variable	Expression
Accumulated Time Step	2540
Current Time Step	2540
L0 crit	$ke^{1.5} / eddy$
LScrit	$L0\ crit / Lmesh$
Lmesh	$Volume^{1/3}$
Reference Pressure	1 [atm]
Sequence Step	2540
Time	5.07 [s]
atstep	Accumulated Time Step
ctstep	Current Time Step
eddy	$(Density * 0.09 * ke^2) / Eddy\ Viscosity$
ke	$0.5 * (Statistical\ Reynolds\ Stress\ uu + Statistical\ Reynolds\ Stress\ vv + Statistical\ Reynolds\ Stress\ ww)$
sstep	Sequence Step
t	Time

Figure 39 Calculation of LScrit



User Defined	
Variable LS crit	
Details of Variable LS crit (scalar)	
Expression	LScrit
Min	8.66242e-07
Max	509.937

Figure 40 Definition of Variable LS crit

Solving CFD models

A CFD model is made up of the mathematic equations that description of the physics (models) we are trying to solve. Due to the complexity of the equations an iterative approach is used. This involves starting with an initial value and then the solver adjusts the values at the nodes until hopefully the equations are solved correctly. The iterative converge of the set of equations on the correct solution is required before the numerical errors in a limited and the model can be used.

Divergence Solution

Abraham00000001.trn model was run forward in time and the model diverged (Figure 41). Divergence means that the solver couldn't even keep trying to solve the model, let alone converged. As a standard industry practice diverged models are not trusted due to their obvious significant numerical errors.

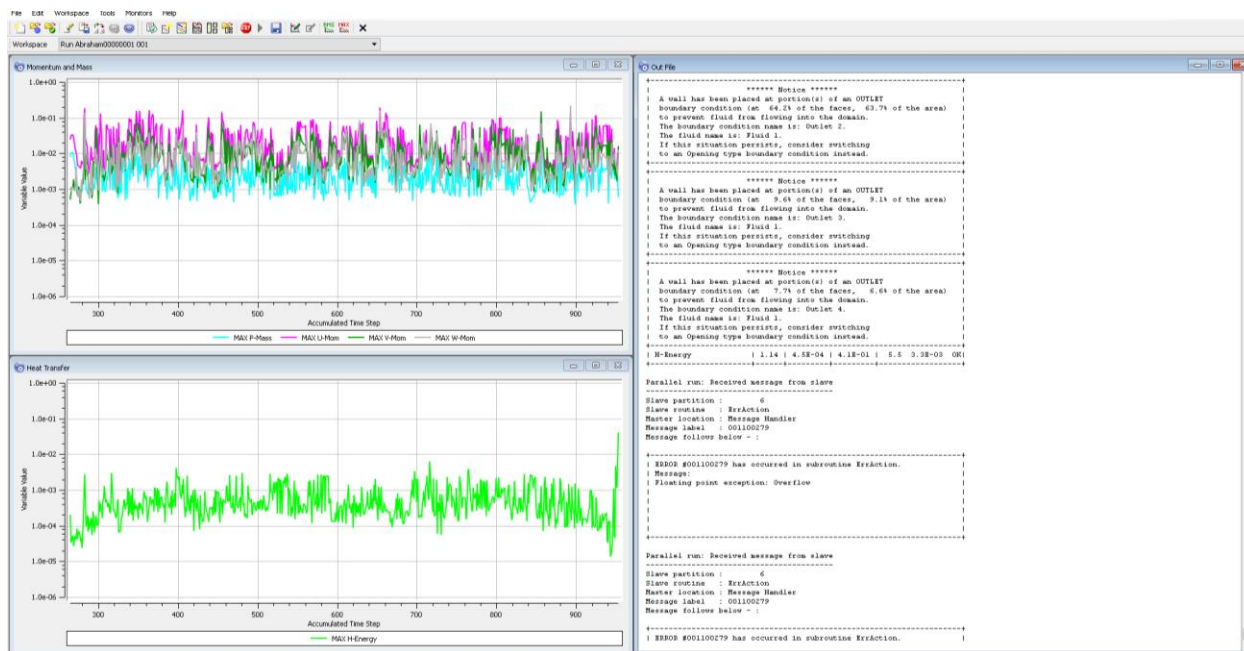


Figure 41 The solution output is shown when the Abraham000001.trn model is run forward. The solver gives a floating point error which indicates the divergence of the model.

1st order accurate

Dr. Abraham makes an error with the 2540_full.trn model by using the High Resolution advection scheme. This is inappropriate for LES turbulence models, the Central Differencing or Bounded Central Differencing scheme should be used. The High Resolution advection scheme is known to result in an inaccurate solution with LES modeling. Figure 42 shows the how the High Resolution Advection Scheme was used. Figure 43 shows the warning produced in the out file when the solver runs the 2540_full.trn file and Figure 44 shows the recommendation from the Ansys Best Practices for Scale-Resolving Simulations in ANSYS CFD Help. Mentor and Egorov state *“No proper LES behaviour can be achieved with an overly dissipative numerical treatment of the convective terms. In industrial LES, the usage of second order central discretisation (CD) schemes is an established technology”*⁶

⁶ The Scale-Adaptive Simulation Method for Unsteady Turbulent Flow Predictions. Part 1: Theory and Model Description F. R. Menter· Y. Egorov


```

****
SOLVER CONTROL:
ADVECTION SCHEME:
  Option = High Resolution
END
CONVERGENCE CONTROL:
  Maximum Number of Coefficient Loops = 10
  Minimum Number of Coefficient Loops = 1
  Timescale Control = Coefficient Loops
END
CONVERGENCE CRITERIA:
  Residual Target = 0.00001
  Residual Type = RMS
END
EQUATION CLASS: momentum
ADVECTION SCHEME:
  Option = High Resolution
END
END
PRESSURE LEVEL INFORMATION:
  Option = Automatic
END
TRANSIENT SCHEME:
  Option = Second Order Backward Euler
TIMESTEP INITIALISATION:
  Option = Automatic
END
END
END
END

```

High Resolution advection scheme

Figure 42 High Resolution setting in 2540_full.trn

```

+-----+
| ERROR #001100279 has occurred in subroutine ErrAction. |
| Message: |
| WARNING: Use of the central difference advection scheme is strong- |
| ly recommended for LES simulations. Another scheme has been used |
| for one or more equation classes. |
| |
| |
+-----+

```

Figure 43 Warning the solver provides with the use of High Resolution with LES model for 2540_full.trn

12.3.1. Spatial Discretization

12.3.1.1. Momentum

SRS models, as described in [Scale-Resolving Simulation \(SRS\) Models – Basic Formulations](#), serve the main purpose of dissipating the energy out of the turbulence spectrum at the limit of the grid resolution. The eddy viscosity is defined to provide the correct dissipation at the larger LES scales. This assumes that the numerical scheme is non-dissipative and that all dissipation results from the LES model. For this reason, one is required to select a numerical scheme in the LES region with low dissipation, relative to the dissipation provided by a subgrid LES model. Another strategy is to avoid the introduction of the LES (subgrid) eddy viscosity and provide all damping through the numerical scheme. This approach is called MILES (Monotone Integrated Large Eddy Simulation) (Boris et al., 1992 [1]). In ANSYS CFD, the standard LES methodology is followed, whereby the dissipation is introduced by a LES eddy viscosity model and the numerical dissipation is kept at a low value.

In order to achieve low numerical dissipation, you cannot use the standard numerical schemes for convection that were developed for the RANS equations (Second Order Upwind Schemes, or SOU), which are dissipative by nature. In contrast, LES is carried out using Central Difference (CD) schemes. In industrial simulations, second order schemes are typically employed, however, in complex geometries with non-ideal grids, CD methods are frequently unstable and produce unphysical wiggles (see [Figure 12.80](#)), which can eventually destroy the solution. To overcome this problem, variations of CD schemes have been developed with more dissipative character, but still much less dissipative than Upwind Schemes. An example is the Bounded Central Difference (BCD) scheme of Jasak et al., 1999 [14].

Figure 44 Recommendation in Ansys Best Practices: Scale-Resolving Simulations in ANSYS CFD

Validation

Dr. Abraham attempts to validate his model based on temperature measurement away from the surgical site, he doesn't show that his model can accurately predict the temperature in the critical region nor that it can accurately predict particle motion, without this any validation claim is limited at best.

Dr. Abraham claims to validate his model, he gives *"the room-averaged temperature was 62°F for an 8.1 million grid-cell calculation"*, however he gives no details of where, when and how his is measuring this value. Without this information it is not possible to evaluate the claim that the models agree with the experimental since the experimental is undefined. Also, the mesh used in his model is not 8.1 million elements as stated, it is unclear if the CFD measurement is from the provided results or not.

Likewise, Dr. Abraham gives a measurement of 60 (°F) 3 inches from the floor. However again he gives no detail of where the measurement was taken. Figures 45 and 46 show the temperature contours 3 inches from the floor. Depending on when, where and how the measurements were taken it is not possible to confirm any agreement between the model result and experimental since significant areas outside of a 59.5 (°F) to 60.5 (°F) range could easily be not in agreement.

Again, the edge of the table agreement claim cannot be evaluated without when, where and how information about the experimental. Also, Figures 47 and 48 shows regions outside the reported range of measurement.

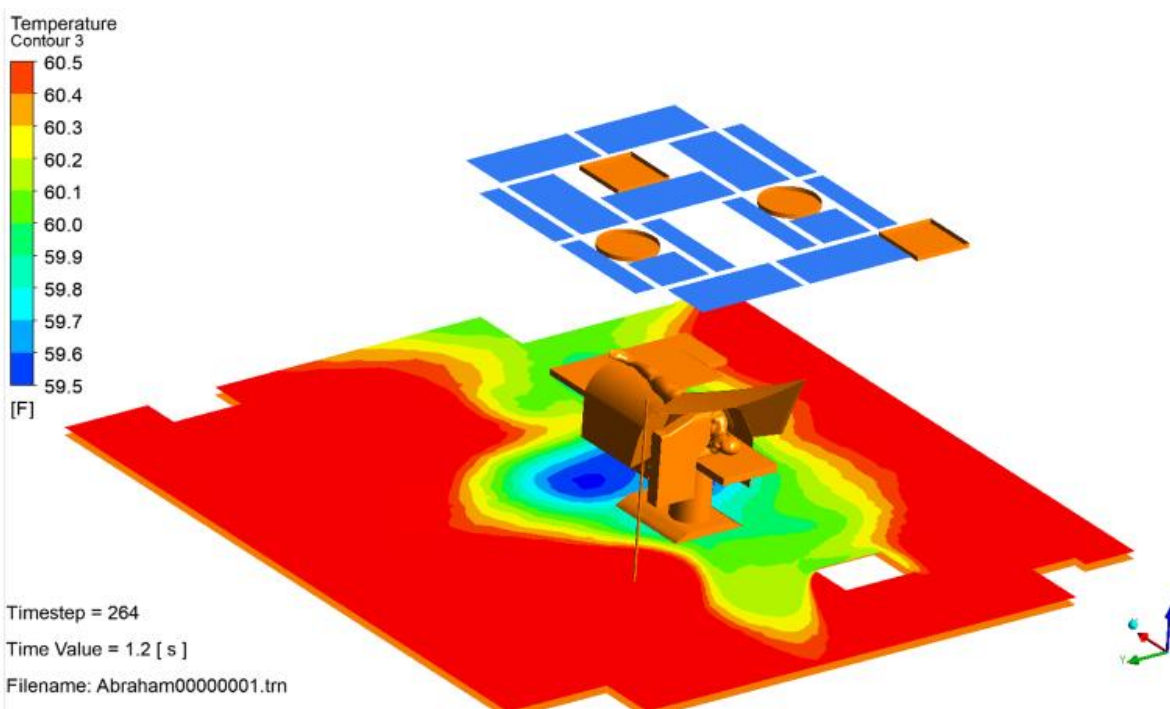


Figure 45 the temperature 3 inch from the floor is show for Abraham00000001.trn. The contours are clipped to between 59.5 (°F) and 60.5 (°F)

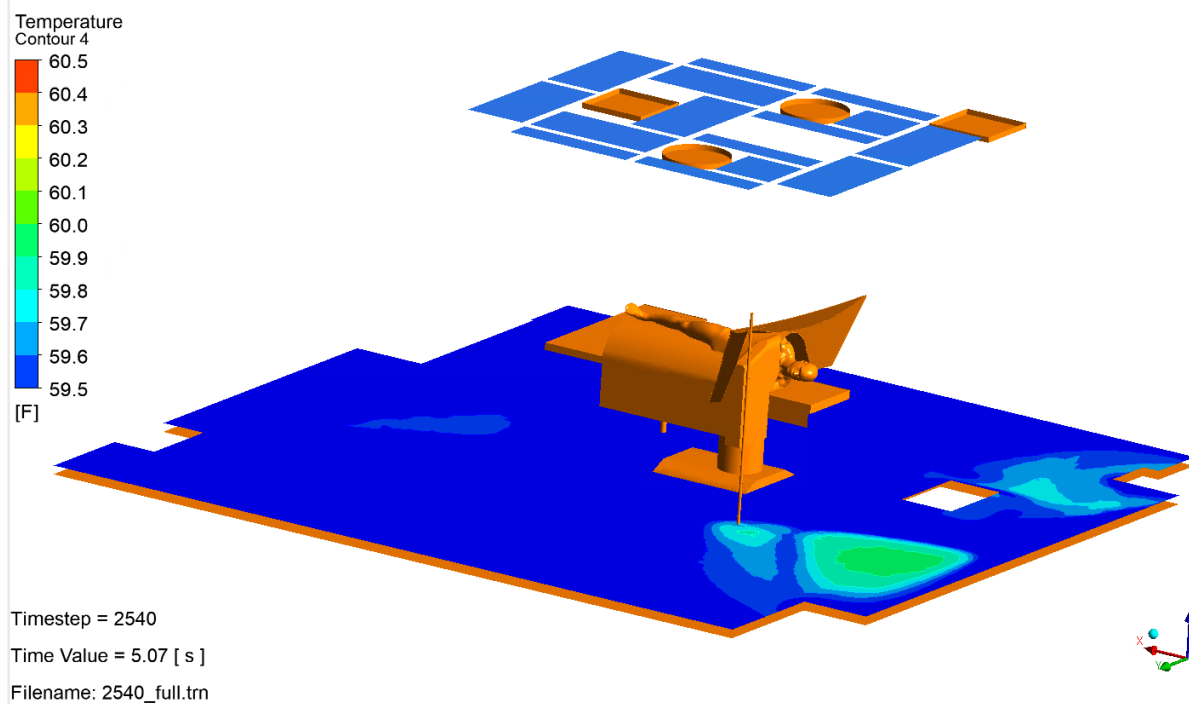


Figure 46 the temperature 3 inch from the floor is show for 2540_full.trn. The contours are clipped to between 59.5 (°F) and 60.5 (°F)

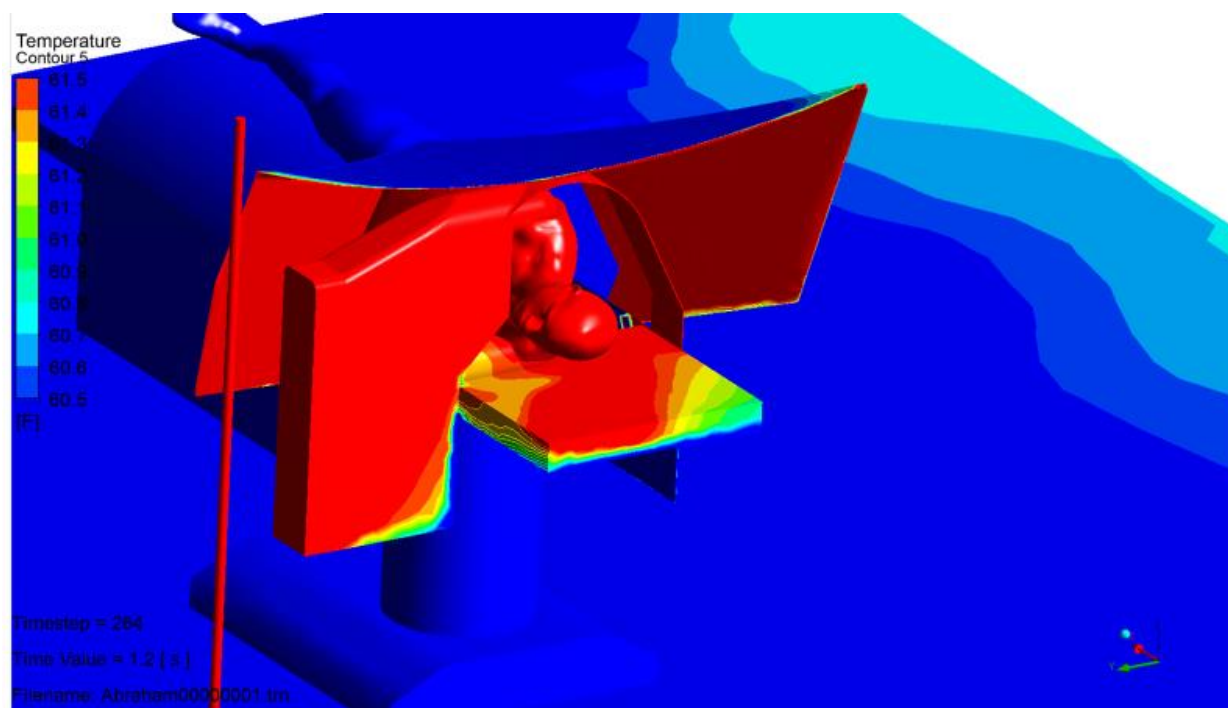


Figure 47 the on the table, drape and body are show for Abraham00000001.trn. The contours are clipped to between 60.5 (°F) and 61.5 (°F)

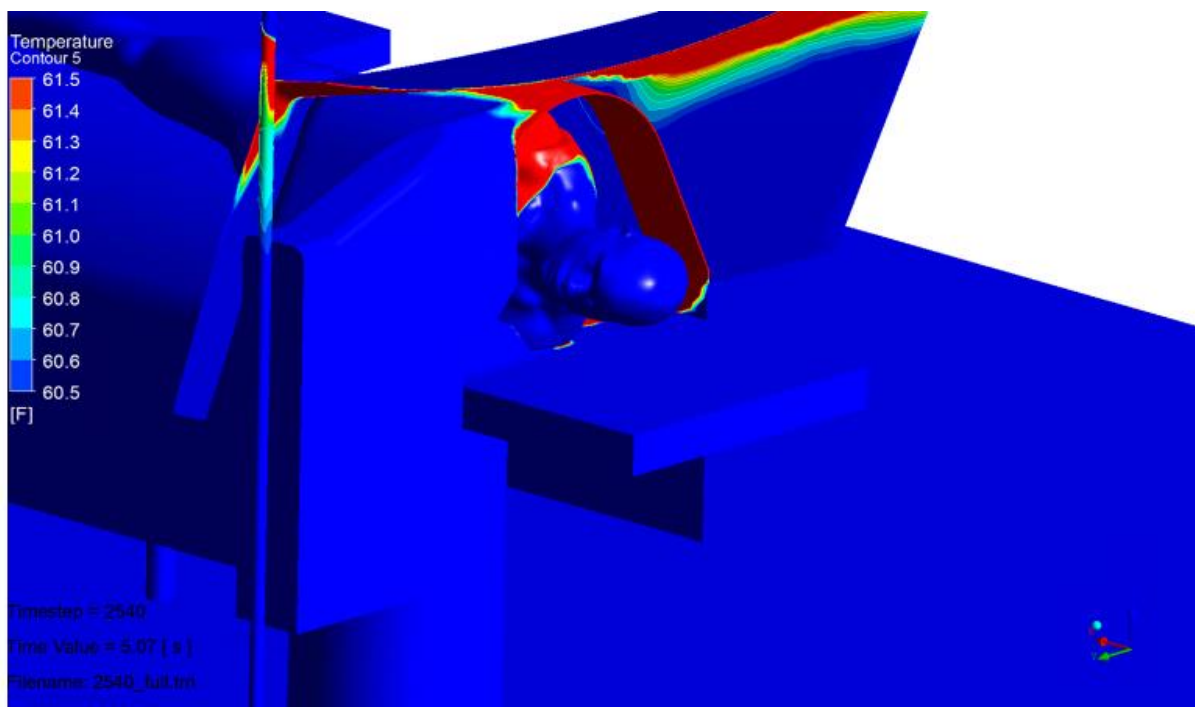


Figure 48 the on the table, drape and body are show for 2540_full.trn. The contours are clipped to between 60.5 (°F) and 61.5 (°F)

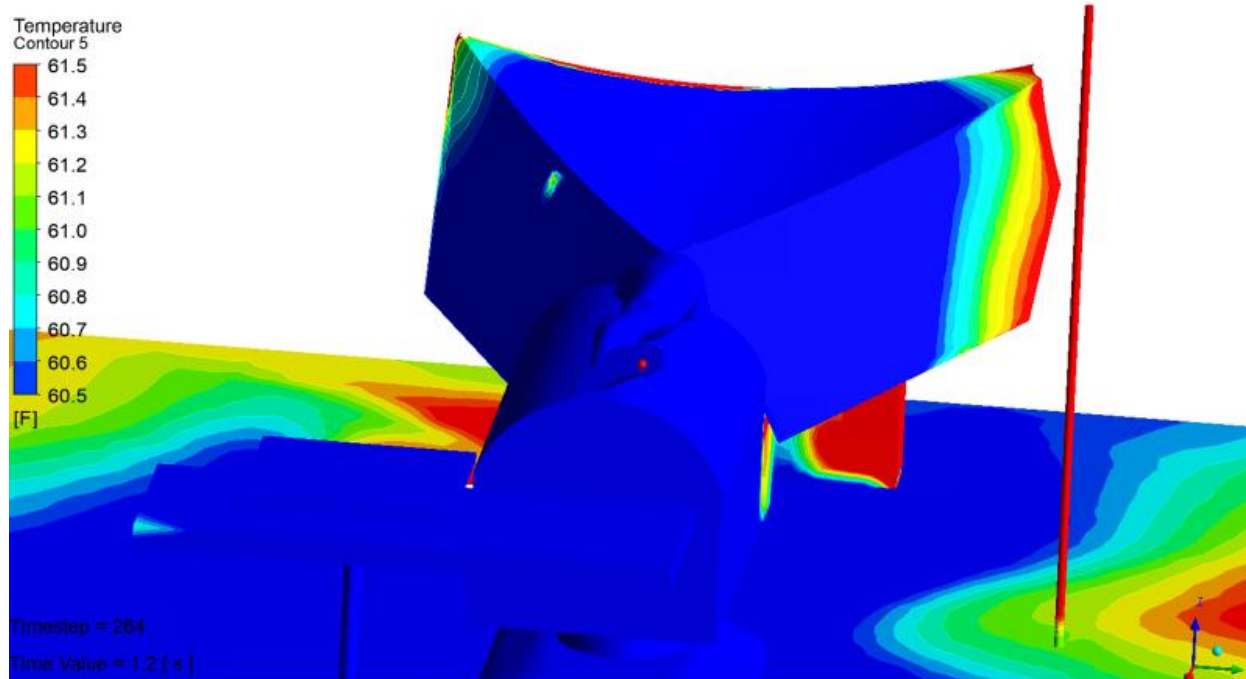


Figure 49 the on the table, drape and body are show for Abraham00000001.trn. The contours are clipped to between 60.5 (°F) and 61.5 (°F)



Lack of Confidence

There are other differences between the model and report, these differences are numerous and there is no discussion or modeling data to support the justification for the changes. This lack of information reduces the confidence that model will capture the true physical situation, given the lack of supporting information to allow reasonable review of his work.

Geometry

Having an accurate geometry in a CFD model is a critical to the correct definition of a CFD model. The results dependent on the shape and size of the geometry used any deviation from the actual geometry will introduce errors.

The geometry used in Dr. Abraham's models is different to the geometry in the report.

The geometry used in Dr. Abraham's models is different to the geometry in the report. The differences include the removal of a number of bodies, changing the dimensions of a body and even adding a body at the end of the surgery table. Figures 51 through 54 show the geometry as report in the report and the actual geometries used.

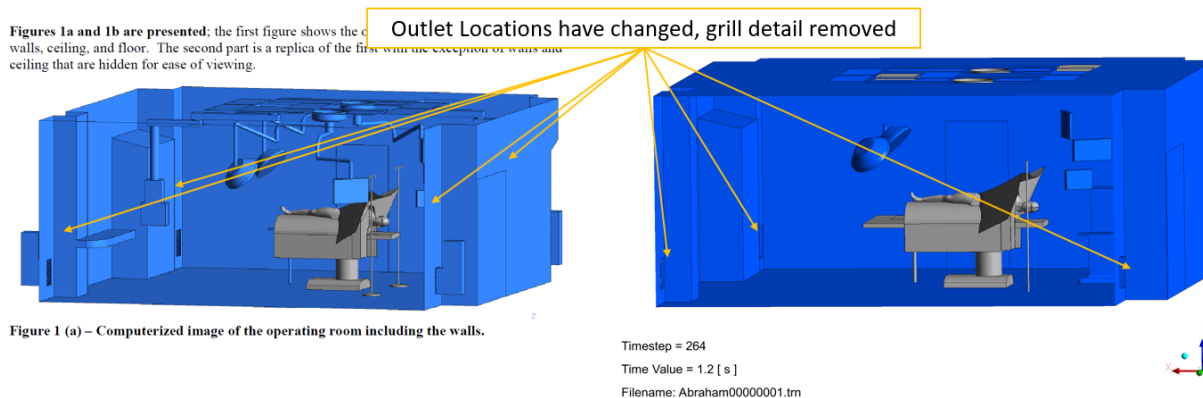


Figure 51 The reported geometry on the left is shown and the actual geometry used in the Abraham00000001.trn model is shown on the right.

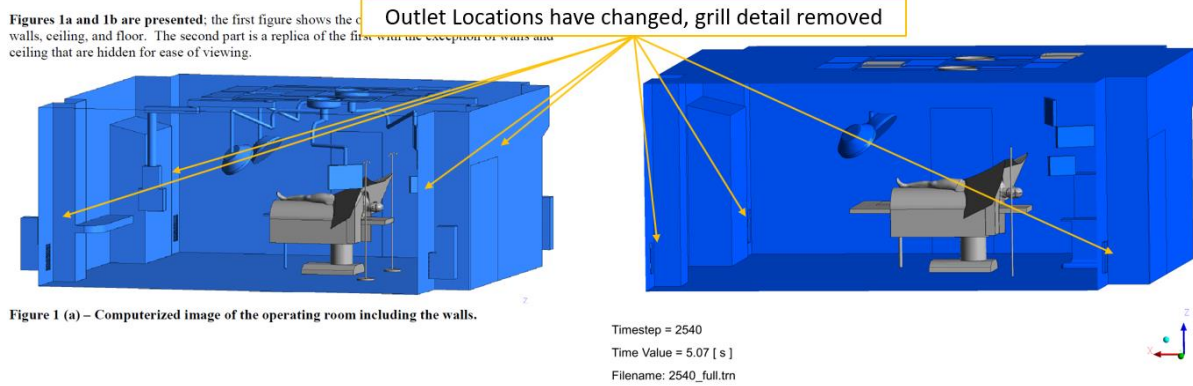


Figure 52 The reported geometry on the left is shown and the actual geometry used in the 2540_full.trn model is shown on the right.

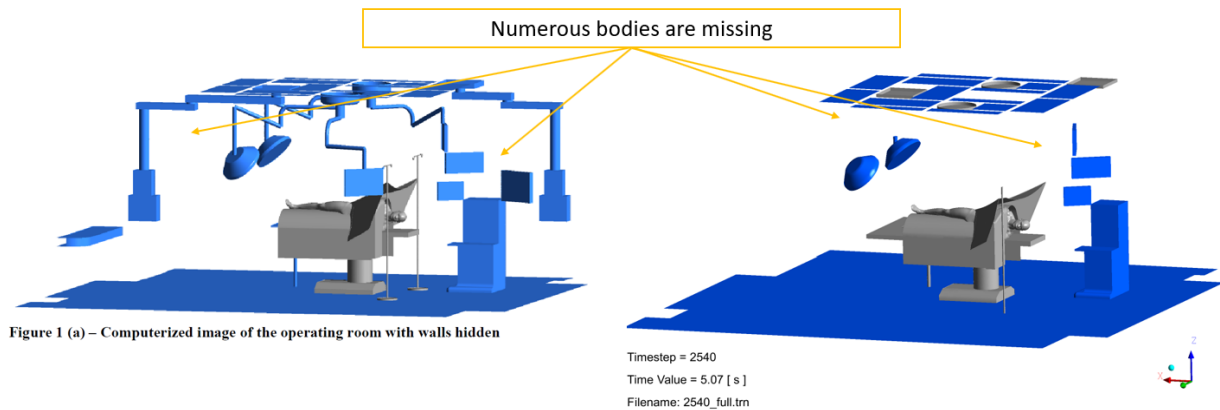


Figure 53 The reported geometry on the left is shown and the actual geometry used in the Abraham00000001.trn model is shown on the right.

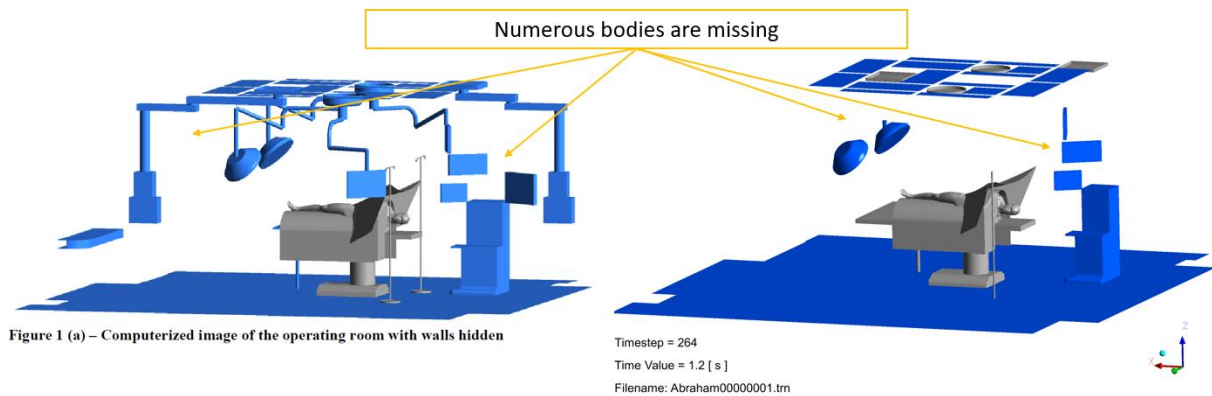


Figure 54 The reported geometry on the left is shown and the actual geometry used in the 2540_full.trn model is shown on the right

Geometry provided is different to the geometry used in the CFD models.

Dr. Abraham, provided a file called Abraham00000003 (2).agdb. The agdb file format is a standard Ansys DesignModeler CAD format. The file contains only one CAD modeling step where a Parasolid file called "D:\3M OR 2015\or-40b-cfd.x_t" is imported.

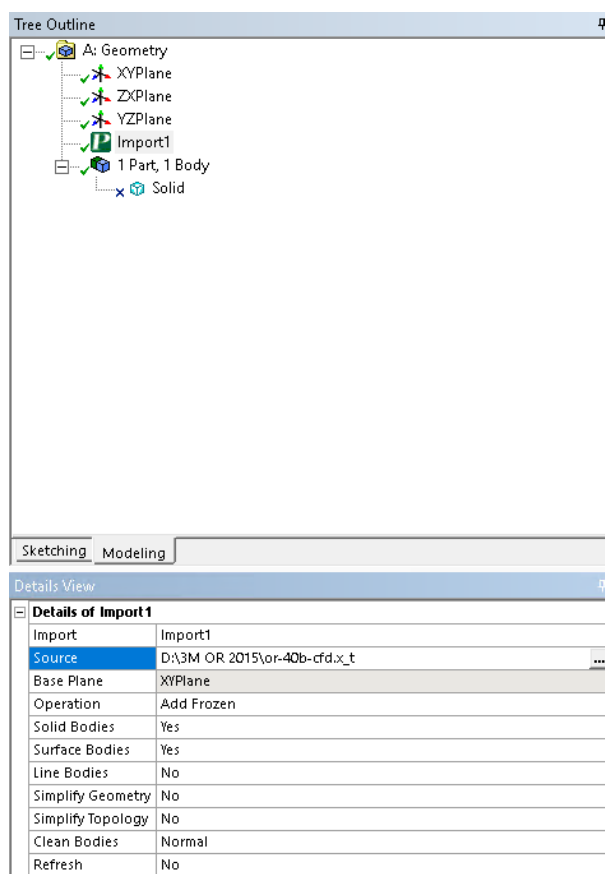


Figure 55 The CAD modeling feature tree is shown for steps are Abraham00000003 (2).agdb

Given the limited information in the report, it appears to be the CAD geometry that is reported in the report which is different to the geometry used in the models. Figures 56 and 57 show how Abraham00000003 (2).agdb is also different to the geometry used in the CFD models. The Abraham00000003 (2).agdb also has the same differences as the reported geometries in the Dr. Abraham's report.

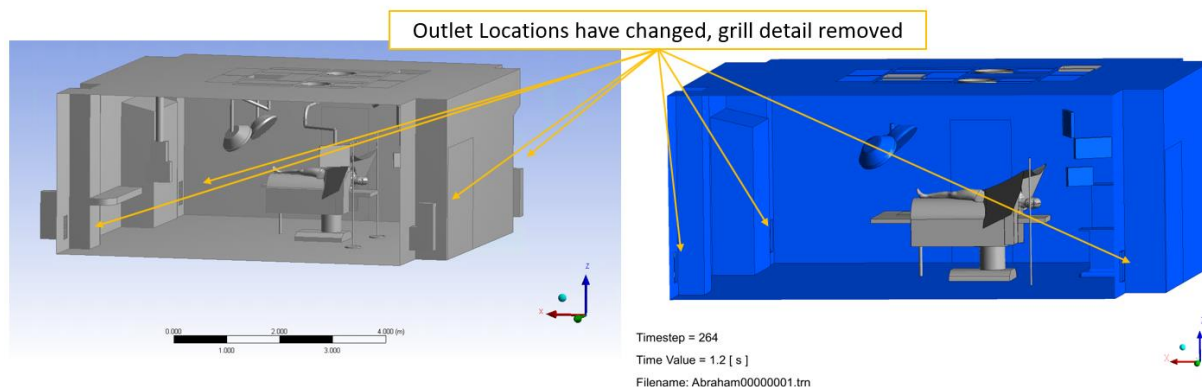


Figure 56 Abraham00000003 (2).agdb CAD geometry (left) is shown beside the model geometry used in Abraham00000001.trn (right)

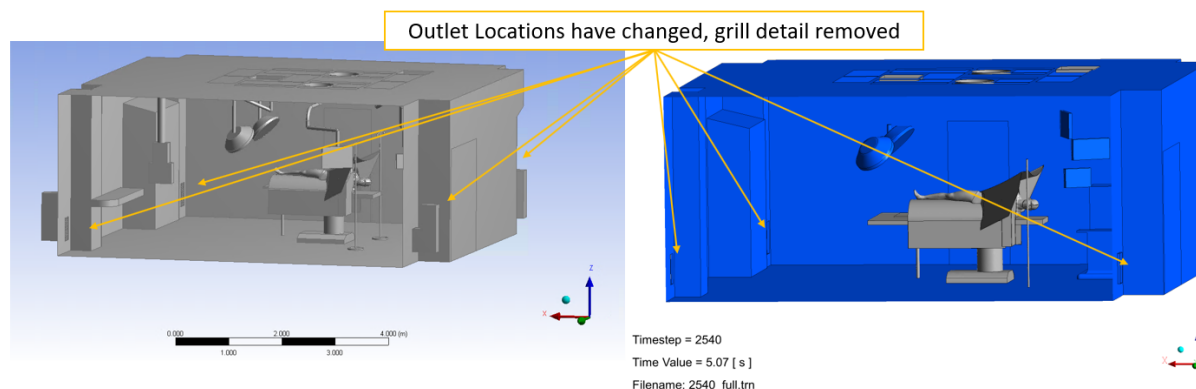


Figure 57 Abraham00000003 (2).agdb CAD geometry (left) is shown beside the model geometry used in Abraham00000001.trn (right)

Bodies were changed in the model.

Because the Abraham00000003 (2).agdb CAD is 3D unlike the 2D pictures, it is possible to further inspect the geometry. It is possible to show a number of additional differences between the CAD and the model geometries. These including the size of the equipment near the head was changed. The when you compare the length of a similar edge the body in the CAD is larger than the body used in the model. Figure 58 show the length an edge on the piece of equipment. Figures 59 and 60 show a line place at the same location and length as CAD edge. The line extends beyond the piece of equipment in the models. Thus, the size of the equipment is different.

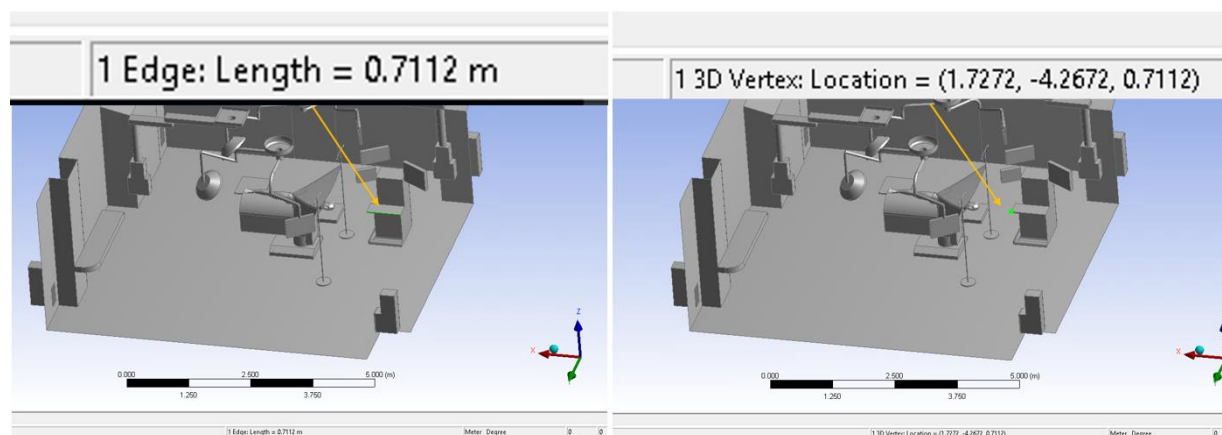


Figure 58 Measured length of edge (left) and vertex (right) location

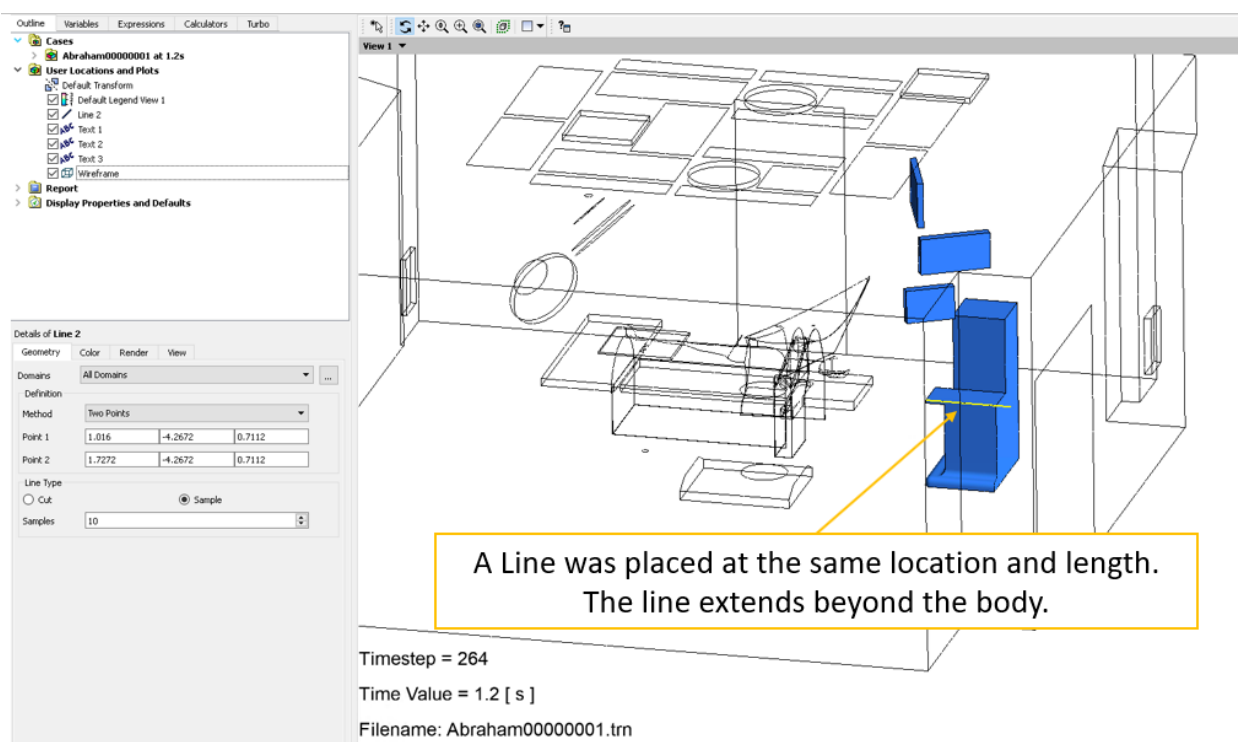


Figure 59 Line placed in same location with 0.7112m length on model the Abraham00000001.trn results.

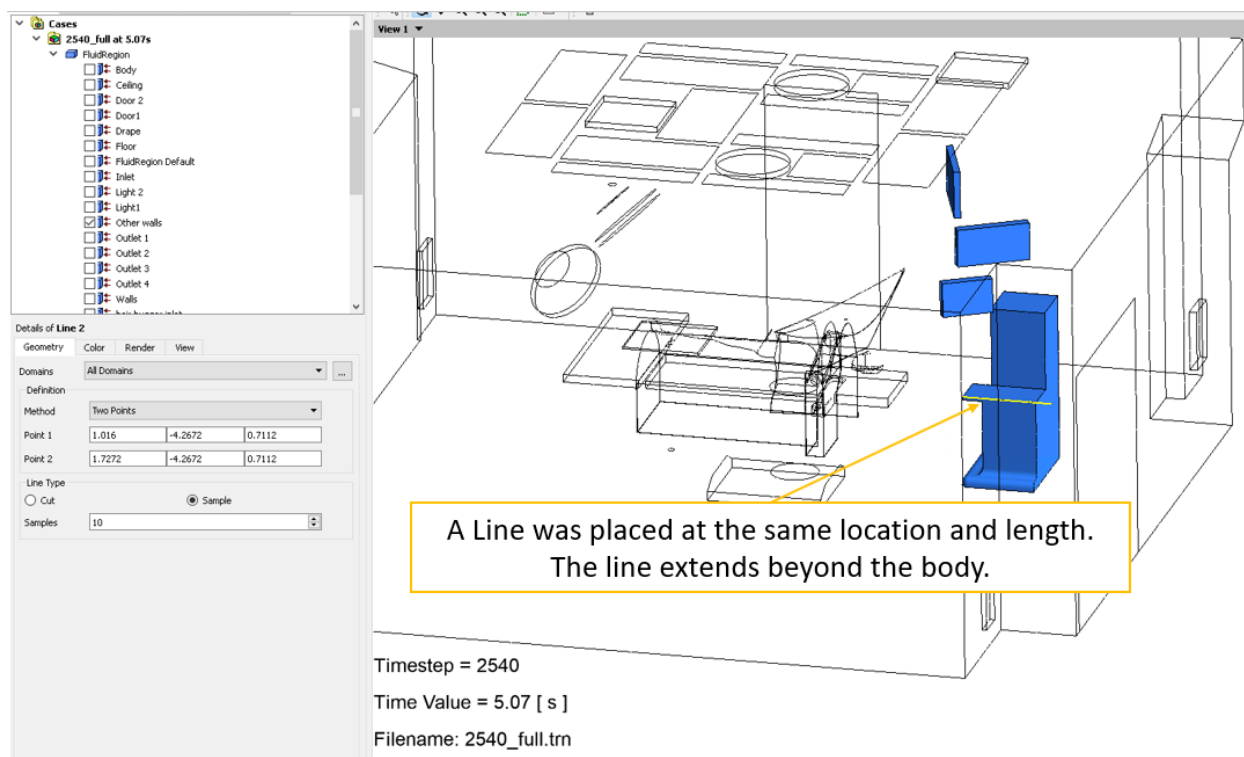


Figure 60 Line placed in same location with 0.7112m length on model 2540_full.trn results.

Bodies were added in the model.

Additionally, Dr. Abraham either changed the shape and size of the table at the feet or added a second connected table, either way results in blocking the floor at the end of the operating table. Figures 61 and 62 show the differences. No justification is given.

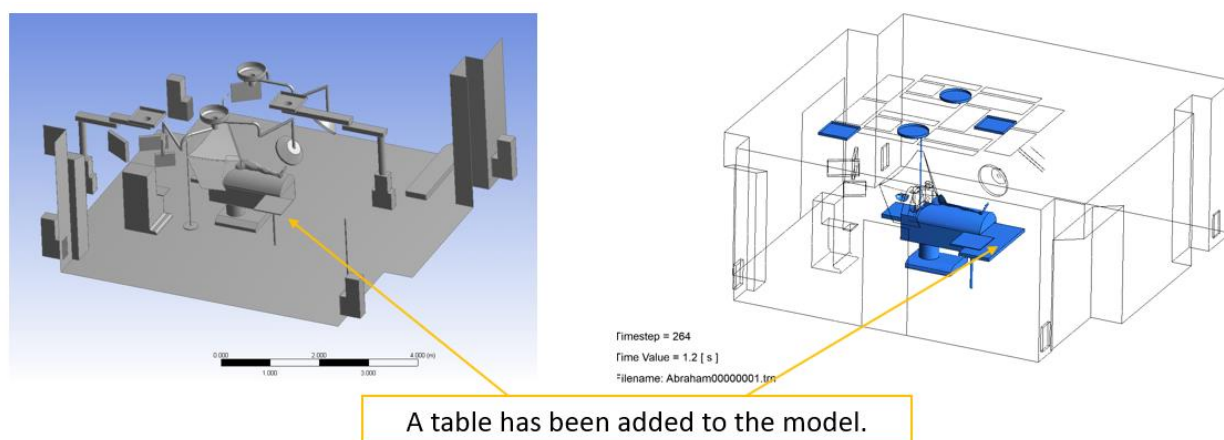


Figure 61 Location of added body not in original CAD but in Abraham00000001.trn CFD model

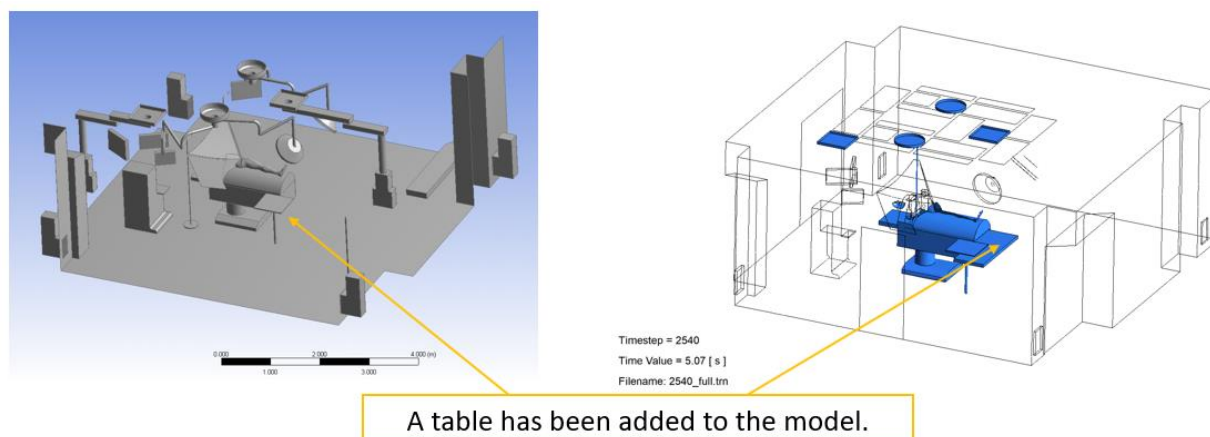


Figure 62 Location of added body not in original CAD but in 2540_full.trn CFD model

The mesh in the model is incorrect compared to the report.

The mesh is shown below for the Abraham00000001.trn (Figure 64) and 2540.trn (Figure 65) is significantly different from the mesh in the report (Figure 63). The mesh is both different because the underlying geometry is different, and the sizing is different. The mesh used, and mesh reported in the report are significantly different.

The mesh in the report appears to be more refined, while the mesh used in the models is coarser than the mesh used shown in the report.

Report

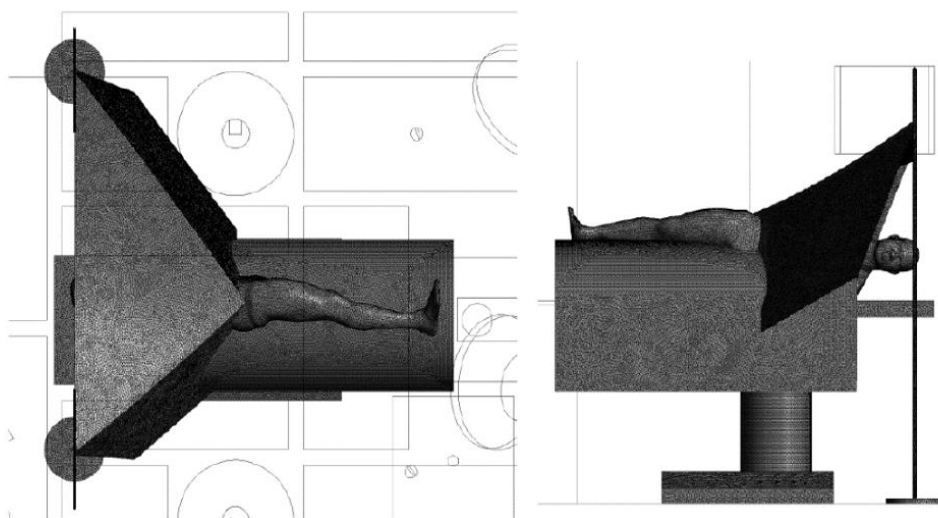


Figure 2 – Images of the cells projected onto the surgical surfaces

Figure 63 is the reported surface mesh used in report

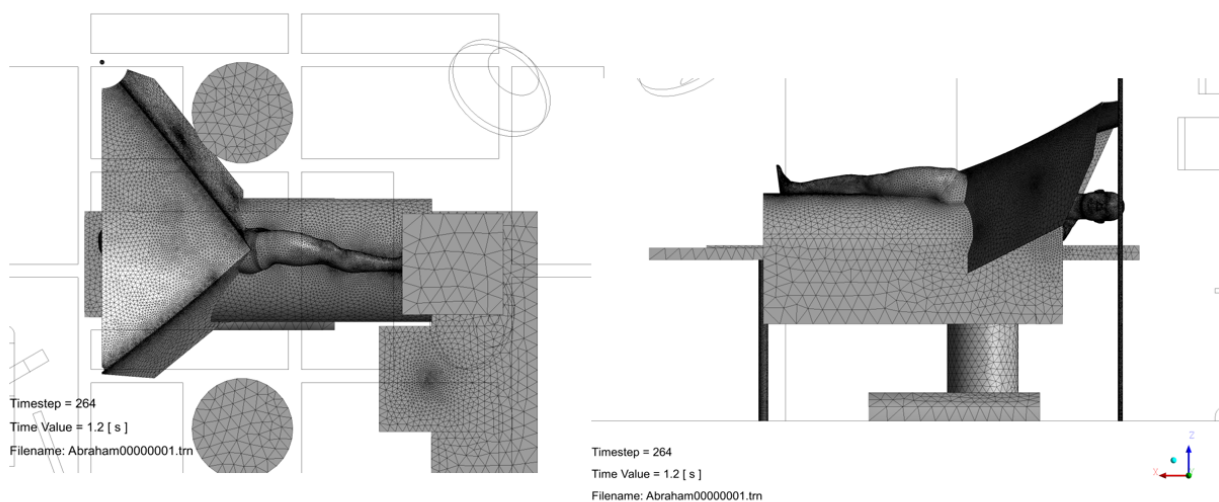


Figure 64 shows the surface mesh used in the Abraham00000001.trn results. The mesh resolution and the underlying bodies that are used to make the mesh are different.

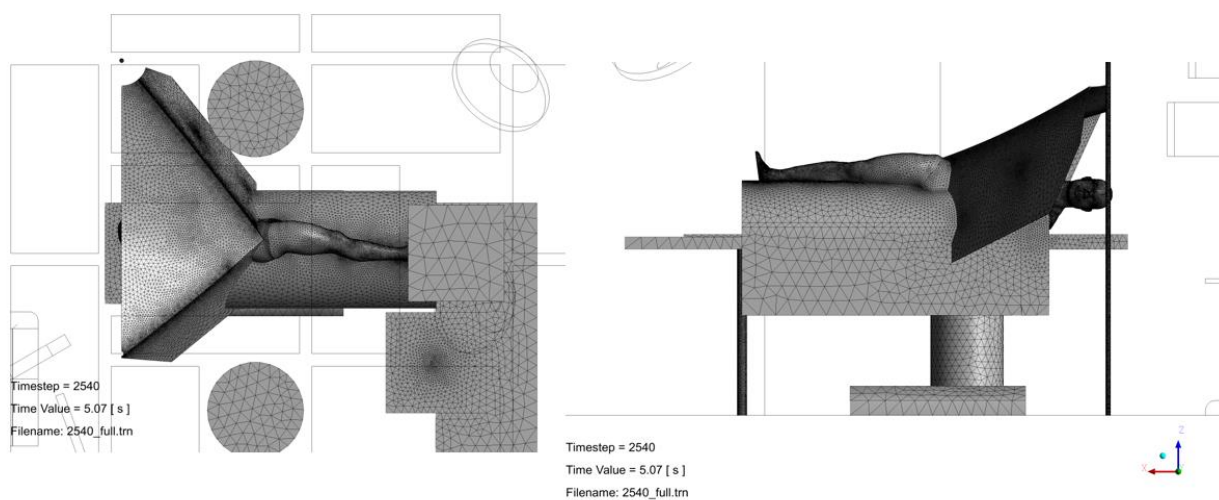


Figure 65 shows the surface mesh used in the 2540_full.trn results. The mesh resolution and the underlying bodies that are used to make the mesh are different.

Mesh count is also different to the report.

Dr. Abraham uses a different mesh size than the one report in his report. He claims “up to 60,000,000 grid cells” in this Step 2 of the analysis – calculation of cells paragraph. He also gives an “for an 8.1 million grid-cell calculation”. Neither are correct the models contain 9.88 million elements and 1.72 million nodes, Figures 66 and 67 for Abraham00000001.trn and 2540_full.trn respectively.

Table 2. Mesh Information for Abraham00000001

Domain	Nodes	Elements
FluidRegion	1718978	9884667

Figure 66 Mesh count information for Abraham00000001.trn

Table 2. Mesh Information for 2540_full

Domain	Nodes	Elements
FluidRegion	1718978	9884667

Figure 67 Mesh count information for 2540_full.trn

Difference Equation of State

Dr. Abraham uses a difference equation of state with his two models. For the Abraham00000001.trn model he uses a constant density of 1.185 (kg m⁻³), for the 2540_full.trn model he uses the ideal gas model. Figure 68 shows the density difference between the two models. Figure 69 shows the density at the inlet, which results in a 3.3% error (Figure 70). Figure 71 shows the velocity at the inlet, which results in a 3.3% error (Figure 72). Figure 73 shows the density at the Bair hugger inlet, which results in a 5.5% error (Figure 74).

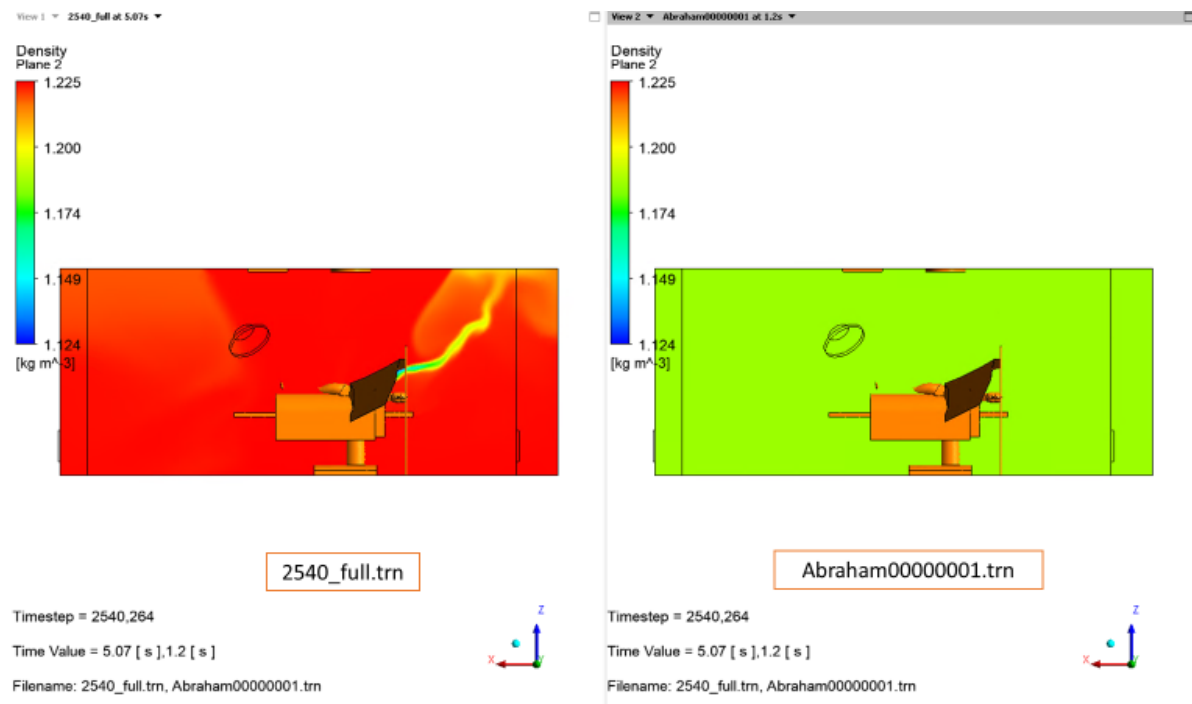


Figure 68 Density at $Y = -3.67143$ (m) for Abraham00000001.trn and 2540_full.trn

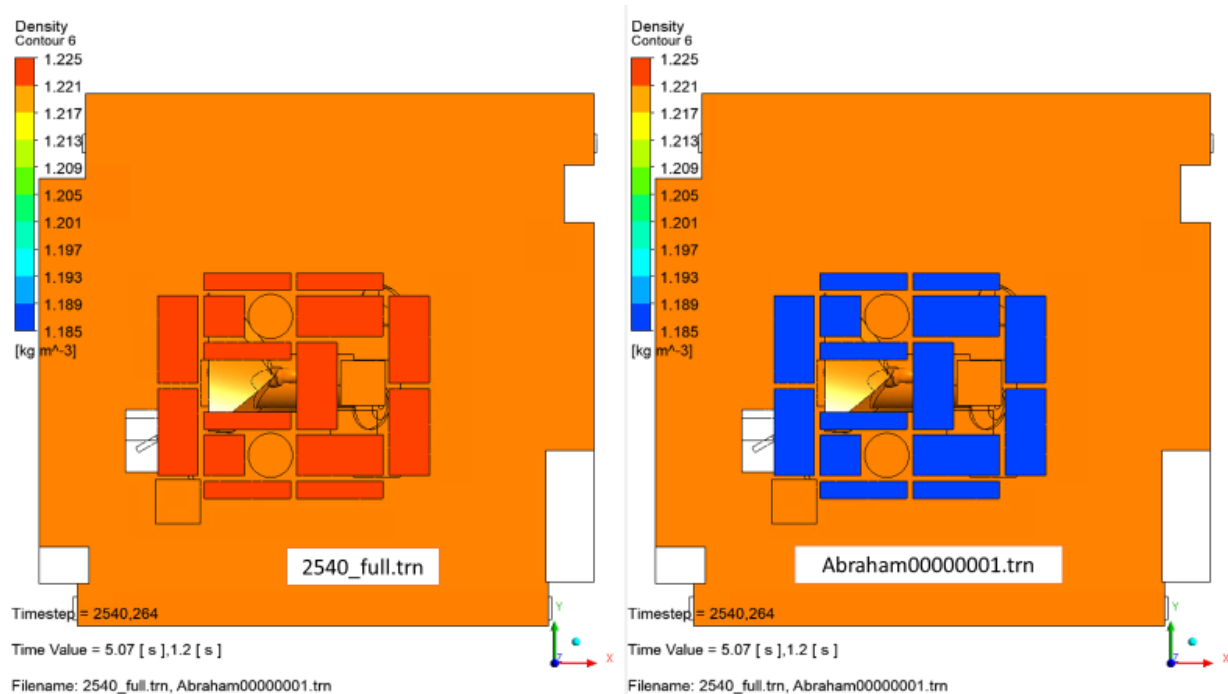


Figure 69 Density at Inlet for Abraham00000001.trn and 2540_full.trn

$$\frac{1.225 \frac{\text{kg}}{\text{m}^3} - 1.185 \frac{\text{kg}}{\text{m}^3}}{1.225 \frac{\text{kg}}{\text{m}^3}} = 3.265\%$$

Figure 70 Calculation of density difference at Inlet between Abraham00000001.trn and 2540_full.trn

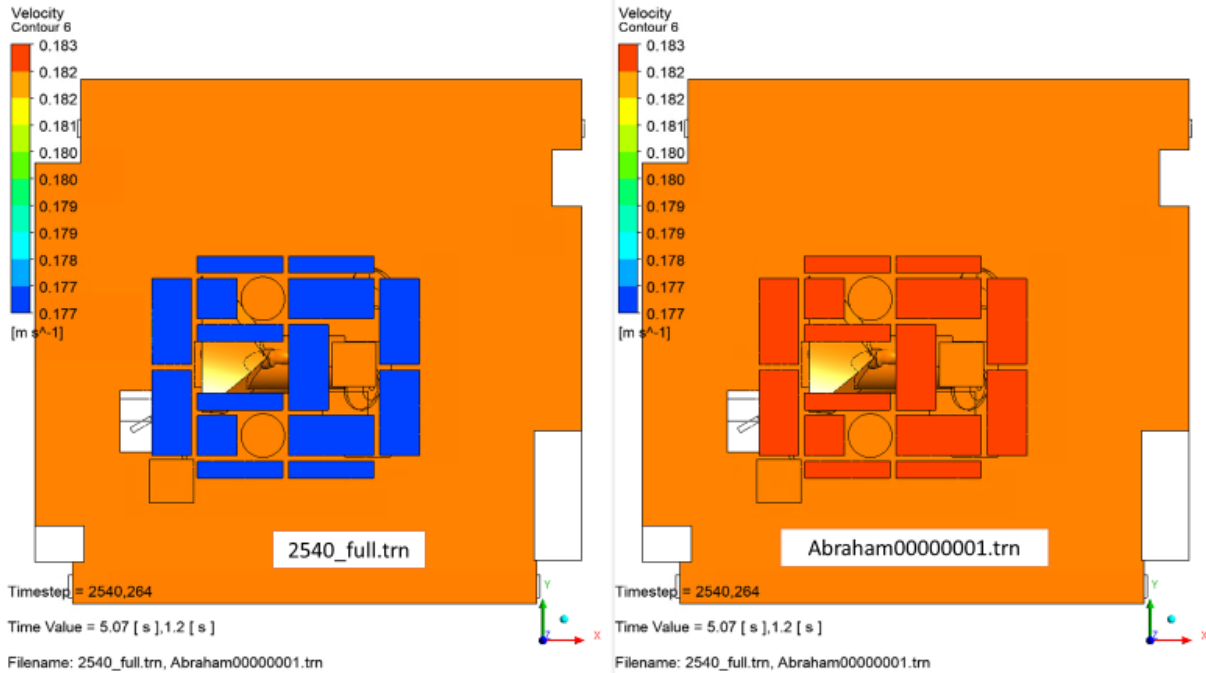


Figure 71 Velocity at Inlet for Abraham00000001.trn and 2540_full.trn

$$\frac{0.183 \frac{\text{m}}{\text{s}} - 0.177 \frac{\text{m}}{\text{s}}}{0.183 \frac{\text{m}}{\text{s}}} = 3.279\%$$

Figure 72 Calculation of velocity difference at Inlet between Abraham00000001.trn and 2540_full.trn

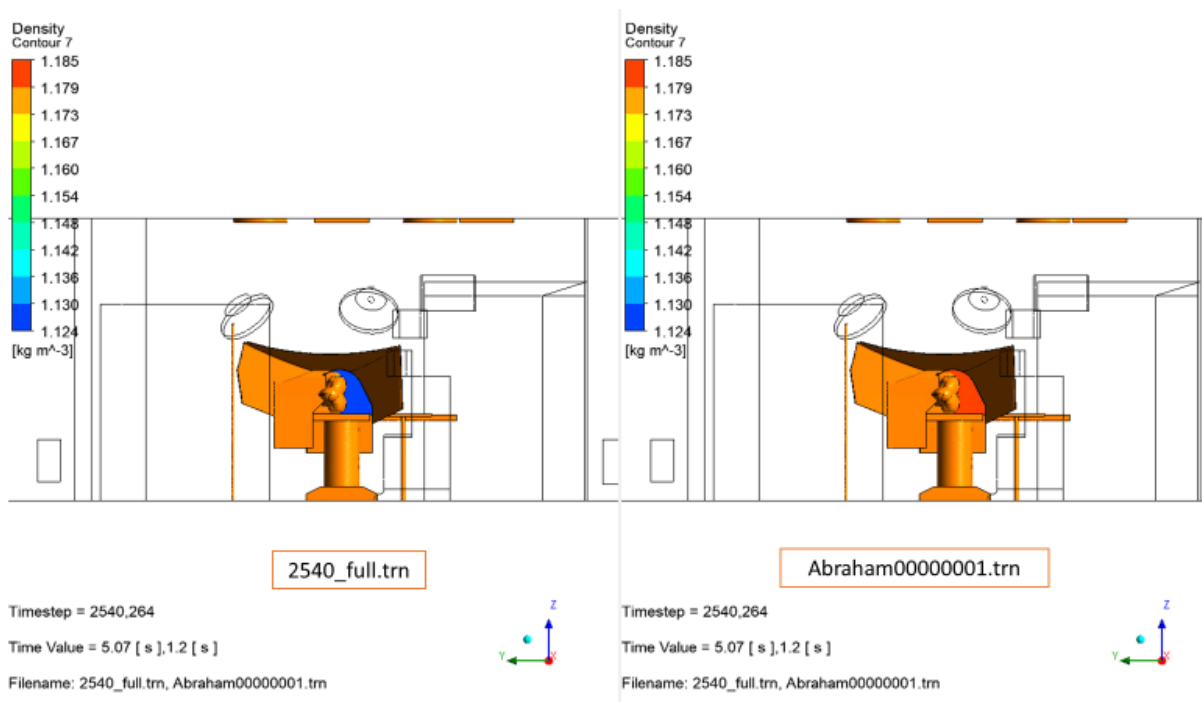


Figure 61 Density at Bair hugger inlet for Abraham00000001.trn and 2540_full.trn

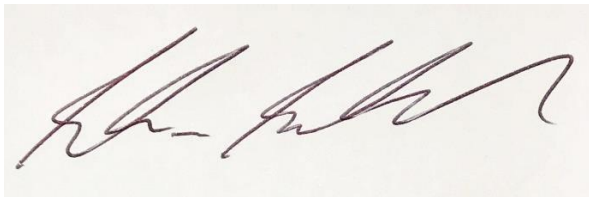
$$\frac{1.12353 \frac{\text{kg}}{\text{m}^3} - 1.185 \frac{\text{kg}}{\text{m}^3}}{1.12353 \frac{\text{kg}}{\text{m}^3}} = -5.471\%$$

Figure 61 Calculation of density difference at Bair hugger inlet between Abraham00000001.trn and 2540_full.trn

Summary

Dr. Abraham CFD modeling does not support his conclusions, there numerous errors in his CFD models. They included:

- Dr. Abraham errors by using a steady state streamline on a single transient result. Streamlines require a steady state solution to be accurate and the transient model Dr. Abraham used is not steady. It can clearly be shown the results will change depending on which result he choose to use.
- Dr. Abraham errors by not running his transient model long enough. He only runs his model for 1.2(s) and 5.07 (s) of simulation time. The model has not had long enough to predict the fluid motion in the operating room as he has defined it. The results can be shown to dependent the definition of his unknown initial condition
- Dr. Abraham uses results from a model that will diverge. This is outside standard industry practices and highly likely to give wrong results.
- Dr. Abraham uses a mesh that is under resolved and has unacceptable quality elements. If he refined his mesh he would get different results.
- Dr. Abraham used a High resolution scheme with his LES which is known to cause errors in the solution.
- Dr. Abraham used streamlines, he should have used particle tracking. Particle tracking is significantly more accurate and the industry standard approach to particle distribution problems.
- Dr. Abraham does not support any of his assumptions with any sensitivity analysis.
- Dr. Abraham's validated is not document enough to be confirmed by his results, also his choice of validation does not prove the accuracy of his methodology of a steady sate streamline on a single transient timestep to accurately particle motion.



Nathan Bushnell, Ph.D.

Appendix I (Resume)

CFD Consulting Engineer

SimuTech Group - Seattle

EDUCATIONAL BACKGROUND

Doctor of Philosophy, Chemical and Process Engineering– University of Canterbury, Christchurch, New Zealand, 2008

Thesis: The Study of Liquid/Vapour Interaction inside a Falling Film Evaporator in the Dairy Industry.

Bachelor of Engineering with honors, Chemical and Process Engineering – University of Canterbury, Christchurch, New Zealand, 1999

Engineering Expertise

- Computational Fluid Dynamics
- Modeling of Multiphase Fluid Flows
- Modeling of Turbulence within complex industrial equipment
- Modeling of Complex Heat Transfer Radiation, Natural Convection and Phase Change

Industry Expertise

- Oil and Gas
- Process Industry
- Consumer Electronics
- Alternative Energy
- Homeland security and Government

PROFESSIONAL EXPERIENCE

CFD Consultant/ Lead Engineer, 2007 –present

SimuTech Group, Everett, WA

- Performed advanced CFD analyses using Ansys FLUENT and Ansys CFX packages.
- Prepared comprehensive technical proposals and secured more than 40 external consulting projects.
- Provide CFD specialized training for professional engineers.
- Provide Project specific training for commercial clients.
- Executed geometry de-featuring and advanced meshing technologies.
- Performed sophisticated post-processing of large CFD data using Ansys Fluent and Ansys CFD-Post packages.
- Provide Technical CFD support for SimuTech Group's industrial customers.

- Provide and present information to SimuTech Group's customers on the state of the art capabilities for Ansys Fluent, CFX and Icepak as new software releases occur.

Sample of Completed Projects:

- Analysis of a novel inline pump for down-hole applications in the oil and gas industry (CFX, Rotating Frame of Reference, Turbulence and Compressible Flow).
- Analysis of the cooling and erosion potential for a spray cooled quench tower (CFX, Steady State, Multiphase, Turbulence and Heat Transfer).
- Mixing and Heating of non-Newtonian Nuclear sludge (CFX, Multiphase, Phase Change, Fluid Structure Interactions).
- Atomization of liquid stream into droplet prior to automated sorting (Fluent, Transient, Multiphase and Laminar).
- Prediction of the collapse of a piston generated underwater cavitation cloud and the resulting acoustic pressure wave (CFX, Transient, Multiphase, Compressible, Turbulence, FSI, Structural Deformation and Stress).
- Simulations of Oil and Gas spills from Pipelines located at the bottom of the sea (FLUENT and CFX, Multiphase, Compressible, Turbulent and Conjugate Heat Transfer).
- Analysis of the fluid flow of a mobile water clarifier for portable clarification of Oil Sand well waste water (CFX, Steady State, Single Phase, MFR and Turbulence).
- Investigation of fluid failure mechanism and redesign of a positive displacement pump used in during fracking process (CFX, Transient, Multiphase, Mesh Deformation and Turbulence).
- Oil sands Steam Assisted Gravity Drainage bitumen recovery and production simulations (CFX, Steady State, Laminar and Porous Media).
- Analysis of the mixing time required for impeller stirred bio reactor tanks (CFX and Fluent, Multiple Frame of Reference, Multiphase, Species Transfer and Turbulence).
- Analysis of an inline mixer pump for down-hole applications in the oil and gas industry (CFX Multiple Frame of Reference, Multiphase and Turbulence).
- Multiple turbine projects, including under water and compressible flows (CFX, FSI, Rotating Frame of Reference Turbulence and Multiphase).
- Analysis of Ring Crystallizer fluid flow (Ansys CFX, Steady State, Porous Medium and Turbulence).
- Analysis of the shear induced cleaning of Solar Tubes under free surface motion (Ansys CFX, Transient, Multiphase and Turbulence).
- Analysis of flow through vibrating ball gate valve (Ansys CFX, Transient, Fluid Structure Interaction, Mesh deformation, incompressible and Turbulence).
- Analysis of biomedical valve (Ansys CFX, Steady State, incompressible and Turbulence).
- Analysis of flow and vibration of an Inline Burner (Ansys CFX, Compressible, Conjugate Heat Transfer, Turbulence and Ansys Mechanical).
- Modeling of a two-stage oxygen regulator (Ansys CFX, Compressible, Conjugate Heat Transfer and Turbulence).

Doctoral Student, 2004–2008

University of Canterbury

- Separation of Droplets inside of an integrated separator (Ansys CFX, Steady and Unsteady flow, Turbulence, Film Atomization and Multiphase).
- Wetting of Milk products on the distribution plate of a falling film evaporator (Ansys CFX, Steady and Unsteady flow, Multiphase and Laminar).

Professional Teaching Experience

CFD Consultant/ Lead Engineer, SimuTech Group

- Taught the Introduction to CFX (4-5day training course) seven times. 2007-present
- Developed and Taught the Ansys CFD short course (1/2 day workshop). 2011-present

Ansys Professional Certification

CFD Consultant/ Lead Engineer

- ANSYS Certified Professional, R19: Fluid Technical
- ANSYS Certified Professional, R18: Fluids – Technical
- ANSYS Certified Professional, R17: Fluids - Technical V1
- ANSYS Certified Professional: Fluids – Technical
- ANSYS Certified Professional: ANSYS Icepak – Technical
- ANSYS Certified Professional, R18: Preprocessing – Technical
- ANSYS Certified Professional, R18: AIM – Technical
- ANSYS Certified Professional: Structural – Technical
- ANSYS Certified Professional: ANSYS AIM – Technical
- ANSYS Certified Professional: ANSYS SpaceClaim - Technical
- 2007 Ansys Fluids Technologies certification for SimuTech Group, Fluent.
 - Certification model: Validation of turbulent flow over repeating hills
- 2011 Recertification SimuTech Group for Ansys CFX
 - Certification model: Turbulent multiphase flow through a positive displacement pump with fluid structure interactions

SPECIAL ACCOMPLISHMENTS AND AWARDS:

Conference Presentations and Journal Papers:

- “A new hybrid heat sink with impinging micro-jet arrays and microchannels fabricated using high volume additive manufacturing”, 2017 33rd Thermal Measurement, Modeling & Management Symposium (SEMI-THERM), Robinson, A.J. and Tan, W. and Kempers, R. and Colenbrander, J. and Bushnell, N. and Chen, R.,
- An ultra high performance heat sink using a novel hybrid impinging microjet — Microchannel structure, Robinson, A.J. and Tan, W. and Kempers, R. and Colenbrander, J. and Bushnell, N. and Chen, R., 2017 16th IEEE Intersociety Conference on Thermal and Thermomechanical Phenomena in Electronic Systems
-

“A single phase hybrid micro heat sink using impinging micro-jet arrays and microchannels”, Robinson, A.J. and Kempers, R. and Colenbrander, J. and Bushnell, N. and Chen, R., Applied Thermal Engineering, Volume 136, May 2018, p408-418

- Presented “Separation of droplets from vapour in the integrated separators of a falling film evaporator” Paper at the 7th World Congress of Chemical Engineering, Glasgow, 2005

National Scholarship Awards:

- Bright Futures Enterprise Ph.D. Scholarship, 2004-2006
- CHEMECA Scholarship, 2005